

A heritable switch in carbon source utilization driven by an unusual yeast prion

Jessica C.S. Brown¹ and Susan Lindquist^{1,2,3}

¹Whitehead Institute for Biomedical Research and Department of Biology, Massachusetts Institute of Technology, Cambridge, Massachusetts 02142, USA; ²Howard Hughes Medical Institute and Department of Biology, Massachusetts Institute of Technology, Cambridge, Massachusetts 02139, USA

Several well-characterized fungal proteins act as prions, proteins capable of multiple conformations, each with different activities, at least one of which is self-propagating. Through such self-propagating changes in function, yeast prions act as protein-based elements of phenotypic inheritance. We report a prion that makes cells resistant to the glucose-associated repression of alternative carbon sources, [GAR⁺] (for “resistant to glucose-associated repression,” with capital letters indicating dominance and brackets indicating its non-Mendelian character). [GAR⁺] appears spontaneously at a high rate and is transmissible by non-Mendelian, cytoplasmic inheritance. Several lines of evidence suggest that the prion state involves a complex between a small fraction of the cellular complement of Pma1, the major plasma membrane proton pump, and Std1, a much lower-abundance protein that participates in glucose signaling. The Pma1 proteins from closely related *Saccharomyces* species are also associated with the appearance of [GAR⁺]. This allowed us to confirm the relationship between Pma1, Std1, and [GAR⁺] by establishing that these proteins can create a transmission barrier for prion propagation and induction in *Saccharomyces cerevisiae*. The fact that yeast cells employ a prion-based mechanism for heritably switching between distinct carbon source utilization strategies, and employ the plasma membrane proton pump to do so, expands the biological framework in which self-propagating protein-based elements of inheritance operate.

[*Keywords:* Prion; yeast; glucose repression; *PMA1*; *STD1*]

Supplemental material is available at <http://www.genesdev.org>.

Received July 1, 2009; revised version accepted August 26, 2009.

The stable inheritance of biological information and phenotype across generations is a fundamental property of living systems. Prions, self-perpetuating and heritable protein conformations that cause multiple phenotypes, represent an unusual mechanism of information transfer that occurs via protein instead of nucleic acid (Wickner 1994). Prion proteins can assume at least two conformations and each conformation alters protein function, resulting in different phenotypes (Wickner et al. 2004; Shorter and Lindquist 2005). When in the self-templating or prion conformation, prion proteins acquire characteristics normally restricted to nucleic acids. The first prion protein identified, the mammalian protein PrP, can behave as a transmissible pathogen and causes a neurodegenerative disease in its prion form (PrP^{Sc}) (Prusiner 1998). Prion proteins in fungi, which are functionally unrelated to PrP and to each other, act as non-Mendelian elements of inheritance by switching to the self-perpet-

uating, cytoplasmically transmissible prion conformation (Wickner 1994).

Four prions have been extensively characterized in fungi: [PSI⁺], [URE3], [Het-s], and [RNQ⁺]. [PSI⁺] (Cox 1965) is the prion form of the translation termination factor Sup35, which causes nonsense suppression (Stansfield et al. 1995; Patino et al. 1996; Paushkin et al. 1996). [URE3] (Lacroute 1971) is an altered form (Wickner 1994) of the nitrogen catabolite repressor Ure2 (Courchesne and Magasanik 1988). [RNQ⁺] controls the ability of a cell to acquire other prions (Derkatch et al. 2000, 2001; Sondheimer and Lindquist 2000). [Het-s], found in *Podospora anserina*, causes heterokaryon incompatibility with certain mating partners (Rizet 1952; Coustou et al. 1997).

These four fungal prions, as well as several recently identified prions ([SWI⁺], [MCA], [OCT⁺], and [MOT⁺]) (Du et al. 2008; Alberti et al. 2009; Nemecek et al. 2009; Patel et al. 2009), share key genetic and physical characteristics despite their disparate functions (Chien et al. 2004; Shorter and Lindquist 2005). Their phenotypes appear spontaneously at higher frequencies than those caused by genetic mutations. They are dominant, show

³Corresponding author.

E-MAIL Lindquist_admin@wi.mit.edu; FAX (617) 258-5737.

Article is online at <http://www.genesdev.org/cgi/doi/10.1101/gad.1839109>.

non-Mendelian segregation following meiosis, and are also transmissible by cytoduction (cytoplasmic transfer). Physically, they form a self-templating amyloid conformation in the $[PRION^+]$ state. Furthermore, their inheritance is linked to the activities of chaperones, proteins that mediate conformational changes in other proteins. Transient changes in chaperone levels, particularly Hsp104, are sufficient to eliminate the prions permanently from cells. This occurs because chaperones alter the prion conformations and transmission to daughter cells. Once the prion template is gone, cells are "cured" of the elements (Uptain and Lindquist 2002; Shorter and Lindquist 2005). Another unusual feature is that transient overexpression of the prion protein causes permanent inheritance of the prion phenotype. This is because the protein::protein interactions involved in prion formation are more likely to occur at higher protein concentrations (Chernoff et al. 1993; Ter-Avanesyan et al. 1993; Wickner 1994; Serio et al. 2000; Sondheimer and Lindquist 2000; Derkatch et al. 2001; Uptain and Lindquist 2002; Shorter and Lindquist 2005). The yeast prions also share a distinctive feature with mammalian prions: a strong transmission barrier across species. Even subtle differences in amino acid sequence can reduce the ability of prion proteins from one species to convert the homolog from other species, even though the homologous protein is itself capable of forming a prion on its own (Aguzzi et al. 2007; Chen et al. 2007).

The precise nature of the mammalian prion template is not known, but all of the well-characterized fungal prions, as well as the newly discovered prions and prion domains (Du et al. 2008; Alberti et al. 2009; Nemecek et al. 2009; Patel et al. 2009), are self-templating amyloid amyloids. The simple and robust character of self-templating amyloids provides a compelling framework for protein-based inheritance (Glover et al. 1997; Shorter and Lindquist 2005). Indeed, in many cases the amyloid has been shown to be the sole determinant needed for prion formation: Recombinant amyloid fibers alone are sufficient to convert $[prion^-]$ cells to $[PRION^+]$ cells (Maddelein et al. 2002; King and Diaz-Avalos 2004; Tanaka et al. 2004; Brachmann et al. 2005; Patel and Liebman 2007; Alberti et al. 2009). Amyloid structure is therefore commonly held to be a critical feature of all naturally occurring systems for protein-based inheritance. Indeed, a recent genome-wide screen for new prion domains in yeast began by examining proteins likely to be amyloidogenic (Alberti et al. 2009).

Here, we took a different approach. We searched the literature for *Saccharomyces cerevisiae* phenotypes with prion-like inheritance patterns. One was described many years ago in a screen for cells with an alteration in carbon source utilization (Ball et al. 1976). The basis of the screen was the extreme preference of *S. cerevisiae* for glucose as a carbon source. In glucose media, cells repress genes necessary to process other carbon sources such as glycerol (Santangelo 2006). Glucosamine, a nonmetabolizable glucose mimetic, induces a similar repression. Therefore, yeast cells cannot use glycerol as a carbon source if even small amounts of glucosamine are present (Hockney and

Freeman 1980; Nevado and Heredia 1996). Some cells spontaneously acquire the ability to use glycerol in the presence of glucosamine, presumably due to defects in glucose repression. Some of these exhibit dominant, non-Mendelian inheritance (Ball et al. 1976). Further, the phenotype is neither carried by the mitochondrial genome nor by a plasmid (Kunz and Ball 1977). Employing a variety of methods, we show here that this factor, $[GAR^+]$ (for "resistant to glucose-associated repression," with capital letters indicating dominance and brackets indicating its non-Mendelian character), exhibits all of the genetic characteristics of a yeast prion, and we use a broad range of biochemical and genetic methods to identify proteins that play a key role in $[GAR^+]$ inheritance.

Results

[GAR⁺] shows non-Mendelian, infectious inheritance

We obtained cells able to use glycerol as a carbon source despite the presence of glucosamine, as did Ball and colleagues (Ball et al. 1976; Kunz and Ball 1977), by selecting for cells that could grow in 2% glycerol in the presence of 0.05% glucosamine. Colonies appeared at a frequency of approximately five in 10^4 cells in the W303 genetic background, well above the predicted mutational frequency (Supplemental Fig. S1). Some recessive mutations allow growth on glycerol in the presence of glucosamine (see Supplemental Table S1; Ball et al. 1976), but the novel phenotypes described by Ball and colleagues (Ball et al. 1976; Kunz and Ball 1977) were dominant. Therefore, we first crossed our cells to wild-type cells. All diploids exhibited an unstable semidominant phenotype (Fig. 1A). Specifically, a mixed population was produced in which some diploids showed "strong" phenotypes (large colonies) and others showed "weak" phenotypes (small colonies) (Supplemental Fig. S2A). Cells with weak phenotypes invariably converted to strong over ~25 generations (data not shown). Notably, both mammalian and fungal prions exhibit "strong" and "weak" strains (Aguzzi et al. 2007).

In yeast, chromosomally inherited traits show 2:2 segregation following meiosis. Both strong and weak $[GAR^+]$ phenotypes, however, exhibited non-Mendelian 4:0 $[GAR^+]:[gar^-]$ non-Mendelian segregation (Fig. 1B). That is, all meiotic progeny exhibited a capacity to grow on glucose in the presence of glucosamine. Spores produced from cells with weak phenotypes generally converted to strong phenotypes (Supplemental Fig. S2B, bottom). We named the responsible genetic element responsible for this trait $[GAR^+]$.

To determine whether $[GAR^+]$ is transmissible by cytoduction (that is, "infectious"), we used a mutant defective in nuclear fusion (*kar1-1*). During mating, *kar1* cells fuse but nuclei do not (Conde and Fink 1976). Selecting for a particular nucleus and cytoplasm of interest after mating accomplishes cytoplasmic exchange without the transfer of nuclear material. We mated a $[GAR^+]$ strain carrying the nuclear markers *URA3⁺ his3⁻* and the cytoplasmic marker ρ^+ to a *kar1-1 [gar⁻]*

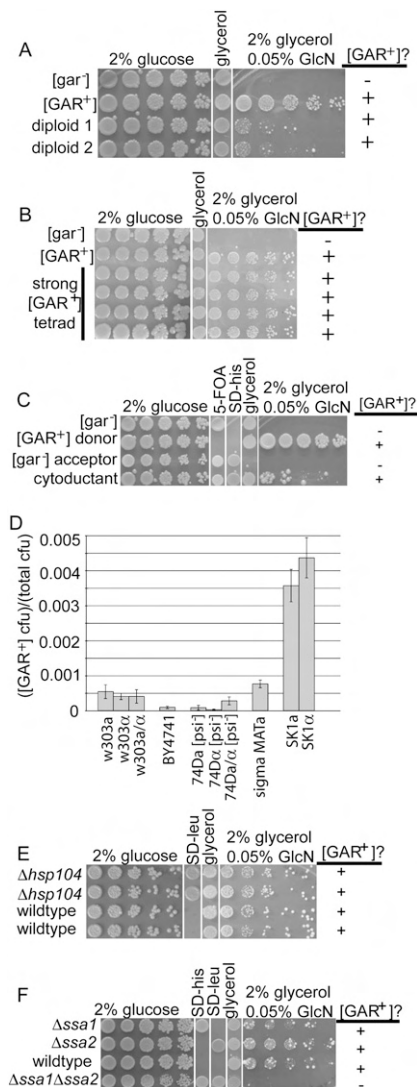


Figure 1. [GAR⁺] shares the genetic characteristics of yeast prions. (A) Mating of [gar⁻] MATα to [GAR⁺] MATα in the W303 background. Resultant diploids show semidominant [GAR⁺] with a mixed population of large colonies (“strong”) and small colonies (“weak”). All spot tests shown are fivefold dilutions. Diploids are selected prior to plating to ensure that they are a pure population. (B) Tetrad spores from the “strong” [GAR⁺]. Diploids in A show non-Mendelian segregation of [GAR⁺]. (C) Cytoduction shows cytoplasmic inheritance of [GAR⁺]. The [GAR⁺] donor is 10B *URA3⁺ his3⁻ ρ⁺ kar1-1* and the acceptor is W303 *ura3⁻ HIS3⁺ ρ⁰ KAR1*. The [GAR⁺] donor is therefore capable of growing on glycerol but the [gar⁻] acceptor is not; “mixed” cells were selected for growth on glycerol ([GAR⁺] cytoplasm) and SD-his 5-FOA ([gar⁻] nucleus and counterselection against the [GAR⁺] nucleus). (D) [GAR⁺] frequency in various laboratory strains. Data are shown as mean ± standard deviation (*n* = 6). (E) Tetrad spores from a [GAR⁺] diploid with the genotype *hsp104::LEU2/HSP104*. Δ*hsp104* spores are still [GAR⁺]. (F) Tetrad spores from a [GAR⁺] diploid with the genotype *ssa1::HIS3/SSA1 ssa2::LEU2/SSA2*. Δ*ssa1*Δ*ssa2* spores are no longer [GAR⁺].

strain that was *ura3⁻ HIS3⁺* and *ρ⁰*. We then selected for cells containing the nucleus originally associated with [gar⁻] cells and the cytoplasm originally associated with [GAR⁺] cells. All 10 strains tested were [GAR⁺] (Fig. 1C). Thus, [GAR⁺] exhibits an “infectious,” nonnuclear pattern of inheritance.

[GAR⁺] appears at high frequency in a variety of genetic backgrounds

We next asked whether [GAR⁺] was an oddity of specific strains or could appear in diverse genotypes. Cells able to use glycerol in the presence of glucosamine appeared at a frequency of approximately nine in 10⁵ cells in the BY background, approximately one in 10⁴ cells in 74D, approximately five in 10⁴ cells in W303, and approximately seven in 10⁴ cells in Sigma. In the SK1 background, [GAR⁺] appeared at the astonishingly high rate of approximately one in 10³ cells (Fig. 1D). In comparison, the frequency of heritable phenotypic change due to genetic mutation is generally approximately one in 10⁶ haploid cells (Ohnishi et al. 2004).

We tested dozens of variants from each background for dominance. All exhibited the semidominant pattern observed in W303 (Fig. 1B; data not shown). [GAR⁺] cells of the 74D background did not sporulate, preventing us from testing segregation pattern. In W303 and W303/BY hybrids, [GAR⁺] only delayed sporulation (data not shown). In every tetrad tested from these backgrounds (>25 of each genotype), [GAR⁺] showed 4:0 [GAR⁺]:[gar⁻] segregation (Fig. 1B; data not shown). Together, these data establish that yeast strains of diverse genetic backgrounds commonly switch carbon utilization strategies in a heritable way by acquiring a non-Mendelian element of inheritance.

[GAR⁺] is curable by transient changes in chaperone protein levels

The inheritance of prions is based on self-perpetuating changes in protein conformations. In contrast to other non-Mendelian elements, a hallmark of prion phenotypes is the ability of transient changes in the expression of chaperones to cause a heritable loss of the phenotype. Other yeast prions, as well as 18 of 19 newly identified protein domains with prion-forming capability, require Hsp104 for propagation (Chernoff et al. 1995; Derkatch et al. 1997; Moriyama et al. 2000; Shorter and Lindquist 2004; Jones and Tuite 2005; Du et al. 2008; Alberti et al. 2009; Patel et al. 2009). To test the influence of Hsp104 on [GAR⁺], we crossed [GAR⁺] cells to cells carrying a knockout of *hsp104* and sporulated them. Hsp104 was not required for [GAR⁺] inheritance: Δ*hsp104* segregants remained [GAR⁺] (Fig. 1E). [GAR⁺] was also not curable by growth on guanidinium hydrochloride, which inhibits Hsp104’s ATPase activity (Ferreira et al. 2001; Jung and Masison 2001), nor by overexpression of *HSP104* (data not shown).

We next tested the Hsp70 proteins Ssa1 and Ssa2 (Werner-Washburne et al. 1987), mutations in which affect the inheritance of other prions (Sweeney and Shorter

2008). These mutations are also a good measure of general chaperone sensitivity, as they induce production of most chaperone proteins (Oka et al. 1997). Strikingly, all Δ ssa1 Δ ssa2 meiotic products lost the ability to grow on glycerol in the presence of glucosamine (Fig. 1F). Was this due to curing of the [GAR⁺] genetic element, or did the Δ ssa1 Δ ssa2 mutations simply mask the phenotype? To test this, we restored SSA1 and SSA2 to the glucosamine-sensitive Δ ssa1 Δ ssa2 progeny by mating them back to wild-type [gar⁻] cells (see Supplemental Fig. S3A for diagram of cross). Restoring Hsp70 function did not result in the reappearance of the [GAR⁺] phenotype (data not shown). However, when the cells were plated on medium with glucosamine, colonies able to grow on glycerol could be recovered at normal frequencies (Supplemental Fig. S3B). Thus, a transient change in chaperone proteins was sufficient to cure cells of [GAR⁺] and this curing was reversible, both hallmarks of prion biology (Wickner 1994). [GAR⁺] therefore exhibits all of the distinguishing genetic characteristics of yeast prions.

[GAR⁺] is regulated by the Rgt2/Snf3 glucose signaling pathway

We performed gene expression profiling to identify transcriptional consequences of [GAR⁺]. In glucose-grown cultures tested just prior to the diauxic shift, only one gene showed a detectable difference between [gar⁻] cells and [GAR⁺] cells on our arrays, but that gene was very strongly affected. Hexose Transporter 3 (*HXT3*) was ~36-fold down-regulated in [GAR⁺] cells compared with [gar⁻] cells (Supplemental Fig. S4). No other transcript exhibited more than a twofold change. We used an Hxt3-GFP fusion protein under the control of the endogenous *HXT3* promoter to examine protein levels. Hxt3-GFP was easily visible at the plasma membrane in late log phase [gar⁻] cells, but extremely difficult to detect in [GAR⁺] cells (Fig. 2A). The loss of *HXT3* expression (Δ hxt3) alone did not allow cells to use glycerol in the presence of glucosamine (Fig. 2B), and thus does not explain the [GAR⁺] phenotype. However, it led us to hypothesize that the causal agent of [GAR⁺] is a regulator of *HXT3* expression.

To define the protein(s) required for [GAR⁺] inheritance, we took advantage of two things. First, transient overexpression of each of the known prion proteins dramatically increases the frequency at which the corresponding prion appears (Uptain and Lindquist 2002). Second, the [GAR⁺] determinant exerts a strong effect on *HXT3* expression, and *HXT3* predominantly controlled by the Snf3/Rgt2 pathway (Kim et al. 2003; Santangelo 2006). When glucose is present, transmembrane glucose sensors Snf3 and Rgt2 transmit a signal to the Yck1 and Yck2 complex, which then phosphorylates Mth1 and Std1, marking them for degradation (Fig. 2C; Moriya and Johnston 2004). When glucose is not present, Mth1 and Std1 accumulate and interact with Rgt1. This complex then binds to the *HXT3* promoter and represses transcription of *HXT3* (Lakshmanan et al. 2003).

We tested each gene in the Snf3/Rgt2 regulatory pathway for induction of [GAR⁺] when overexpressed

from a plasmid with a strong constitutive promoter, GPD (Fig. 2D). In every strain test, *STD1* caused an extraordinary increase in the appearance of colonies able to grow on glycerol in the presence of glucosamine. In W303, for example, the increase was ~900-fold over empty vector; more than one in 10 cells in these cultures converted to [GAR⁺]. This is at the high end of prion inductions obtained by analogous experiments with other proteins (Masison and Wickner 1995; Derkatch et al. 1996). While no other gene in this pathway induced [GAR⁺], overexpression of the *STD1* paralog *MTH1* blocked its appearance, further confirming the importance of members of this pathway in [GAR⁺] biology.

Transient *STD1* overexpression induces [GAR⁺] but is not required for maintenance

Next, we asked if transient expression of *STD1* was sufficient to create a heritable change in phenotype, a defining feature of prion biology. When ~100 cells that had lost the overexpression plasmid were tested, all retained the [GAR⁺] phenotype (confirmed by marker loss) (data not shown). Thus, *STD1* is not simply a dynamic regulator of glucose repression. Rather, its transient overexpression induces a new, heritable state of carbon utilization.

These data suggested that Std1 is the determinant of the [GAR⁺] prion, but further data indicated it could not be the sole determinant. First, most prion phenotypes mimic loss-of-function phenotypes of their prion determinants. However, Δ std1 strains derived from a [gar⁻] background were not able to grow on glycerol in the presence of glucosamine (Fig. 2B; data not shown). Furthermore, Δ std1 cells derived from a [GAR⁺] background were able to do so, indicating that they kept the prion (data not shown). Finally, such cells were able to pass the [GAR] element onto progeny in tester crosses for inheritance of the prion element (Fig. 2E). Therefore, [GAR⁺] maintenance does not require *STD1*. This makes [GAR⁺] highly unusual among yeast prions in that its transient inducing agent is not required for propagation.

We next examined all other members of the Rgt2/Snf3 pathway. None behaved as would be expected for the causal agent of [GAR⁺]. All knockouts were capable of propagating [GAR⁺] (Supplemental Fig. S5). Cells with *rgt1* knockouts did not exhibit the prion phenotype, but they maintained it in a "cryptic" form. It reappeared when cells were crossed to [gar⁻] *RGT1* cells. Therefore, *RGT1* is required for the manifestation of the [GAR⁺] phenotype but is not necessary for its propagation.

Identification of genes that modify the frequency of [GAR⁺] appearance

We conducted genome-wide screens for affectors of [GAR⁺] induction. We screened the *S. cerevisiae* haploid deletion library (Giaever et al. 2002) for mutants that were incapable of inducing [GAR⁺] (Supplemental Table S2), caused a high frequency of appearance of [GAR⁺] (Supplemental Table S3), or that themselves exhibited an ability to grow on glycerol in the presence of glucosamine

Brown and Lindquist

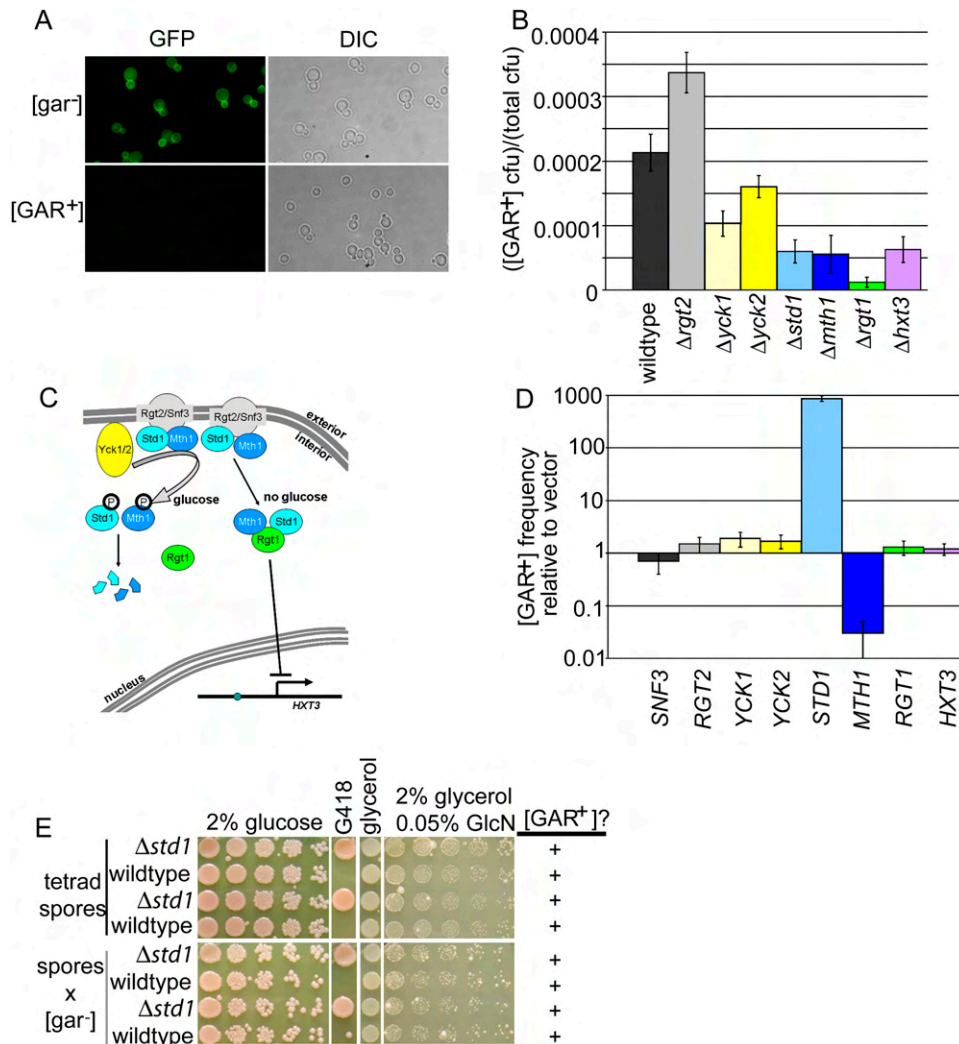


Figure 2. The Snf3/Rgt2 glucose signaling pathway affects [GAR⁺]. (A) Hxt3-GFP signal in [gar⁻] and [GAR⁺] cells (S288c background) by fluorescence microscopy. (B) Frequency of [GAR⁺] in knockouts of members of the Snf3/Rgt2 glucose signaling pathway. $\Delta snf3$ is completely resistant to glucosamine, and therefore [GAR⁺] frequency could not be measured. Furthermore, the frequency of spontaneous glucosamine-resistant colonies in the $\Delta rgt1$, $\Delta std1$, and $\Delta mth1$ strains was close to the rate of genetic mutation, and therefore these colonies might not carry the actual [GAR⁺] element. Overall, this pathway is enriched for genes that alter [GAR⁺] frequency when knocked out relative to the library of nonessential genes ($P = 8 \times 10^{-6}$, Fisher's exact test). (C) The Snf3/Rgt2 glucose signaling pathway. (Adapted with permission from Moriya and Johnston 2004; ©2004 National Academy of Sciences, USA.) (D) Measurement of [GAR⁺] frequency following overexpression of Snf3/Rgt2 pathway members. Data are shown as mean \pm standard deviation ($n = 6$). *STD1* strongly induces conversion to [GAR⁺] and *MTH1* blocks it. (E, top) Tetrad spores from a [GAR⁺] diploid with the genotype *std1::kanMX/STD1*. (Bottom) Spores from *top* crossed to a [gar⁻] strain with a wild-type *STD1* allele.

(Supplemental Table S1). Four of the eight members of the Snf3/Rgt2 pathway showed a phenotype in this screen ($P = 8 \times 10^{-6}$; Fisher's exact test). $\Delta snf3$ grows on glycerol with glucosamine (Supplemental Table S1), and $\Delta std1$, $\Delta mth1$, and $\Delta rgt1$ exhibited lower than normal [GAR⁺] induction (Fig. 2B; Supplemental Table S2). However, none of these genes were required for the maintenance of [GAR⁺] in strains already carrying the element (Supplemental Fig. S5).

Finally, we screened a library of ~5000 ORFs (~85% of yeast ORFs) on a galactose-inducible single-copy plasmid (Leonardo et al. 2002) to find genes that induce [GAR⁺] following overexpression. *STD1* was the only clone that

caused strong [GAR⁺] induction, ~1000-fold when retested under the regulation of the *GPD* promoter. A second gene, *DOG2*, caused a 10-fold induction (Supplemental Fig. S6).

Pma1 associates with *Std1* and is a component of [GAR⁺]

Since neither the deletion nor the overexpression screen identified a protein that by itself could embody the [GAR⁺] prion, we turned to biochemical methods. *STD1* had been implicated in [GAR⁺] in three ways: (1) The highly specific down-regulation of *HXT3* pointed to

members of the Rgt2/Snf3 glucose signaling pathway, (2) transient *STD1* overexpression caused huge increases in $[GAR^+]$ appearance, and (3) deletion of *std1* reduced the spontaneous appearance of $[GAR^+]$ to the frequency of genetic mutations. We hypothesized, therefore, that Std1 might physically interact with an unknown propagating agent.

We sought proteins that interacted with Std1 by coimmunoprecipitation with an HA-tagged derivative. A high-molecular-weight (HMW) band was recovered from $[GAR^+]$ protein lysates but not from $[gar^-]$ lysates (Supplemental Fig. S7). Mass spectrometry analysis identified the protein as Pma1, a large, highly abundant P-type ATPase with 10 transmembrane domains that is the major controller of membrane potential and cytoplasmic pH (Morsomme et al. 2000). When the same assay was performed with isogenic $\Delta std1$ cells, Pma1 was not detected. Notably, if Pma1 is indeed a constituent of the prion, we would not have identified it in our genetic screens. It is essential (Serrano et al. 1986), and therefore it is absent from the deletion library. Moreover, it is already the most abundant membrane protein in yeast and is notoriously difficult to overexpress (Eraso et al. 1987).

Transient overexpression of *STD1* induced $[GAR^+]$ and transient overexpression of its paralog, *MTH1*, inhibited $[GAR^+]$ conversion. We therefore asked whether Pma1 exhibited heritable differences in association with Std1

and Mth1 in $[gar^-]$ and $[GAR^+]$ cells. As a multipass transmembrane protein, Pma1 is intractable to most methods of analyzing protein complexes, but it migrates as an oligomeric species when digitonin lysates are separated on Blue Native gels (Gaigg et al. 2005). Most Pma1 in $[GAR^+]$ and $[gar^-]$ cells migrated as heterogeneous HMW complexes, but a smaller fraction migrated as two distinct complexes of (very roughly) 600 and 700 kDa (Fig. 3A, top). The lower bands (especially the 600-kDa species) were associated with Std1 in $[GAR^+]$ cells but with Mth1 in $[gar^-]$ cells (Fig. 3A, bottom). Std1 is much less abundant than Pma1. Consistent with the fact that only a small fraction of Pma1 is associated with Std1 in $[GAR^+]$ cells, Pma1 showed a minor but statistically significant change in protease sensitivity between $[gar^-]$ and $[GAR^+]$ cells (Supplemental Fig. S8).

Next, we asked whether mutations that affect Pma1 oligomerization and trafficking to the plasma membrane alter $[GAR^+]$ frequency. Mutants that affect phospholipid synthesis and protein trafficking but not Pma1 oligomerization—*LCB3*, *LCB4*, *DPL1*, and *ATG19* (Lee et al. 2002; Mazon et al. 2007)—did not change the appearance of $[GAR^+]$ (Fig. 3B; Supplemental Fig. S9A). Mutants that do affect Pma1 oligomerization and trafficking—*SUR4* and *LST1* (Roberg et al. 1999; Lee et al. 2002)—decreased the appearance of $[GAR^+]$ (Fig. 3B; Supplemental Fig. S9A). These genes were not, however, required for $[GAR^+]$ maintenance (Supplemental Fig. S9B).

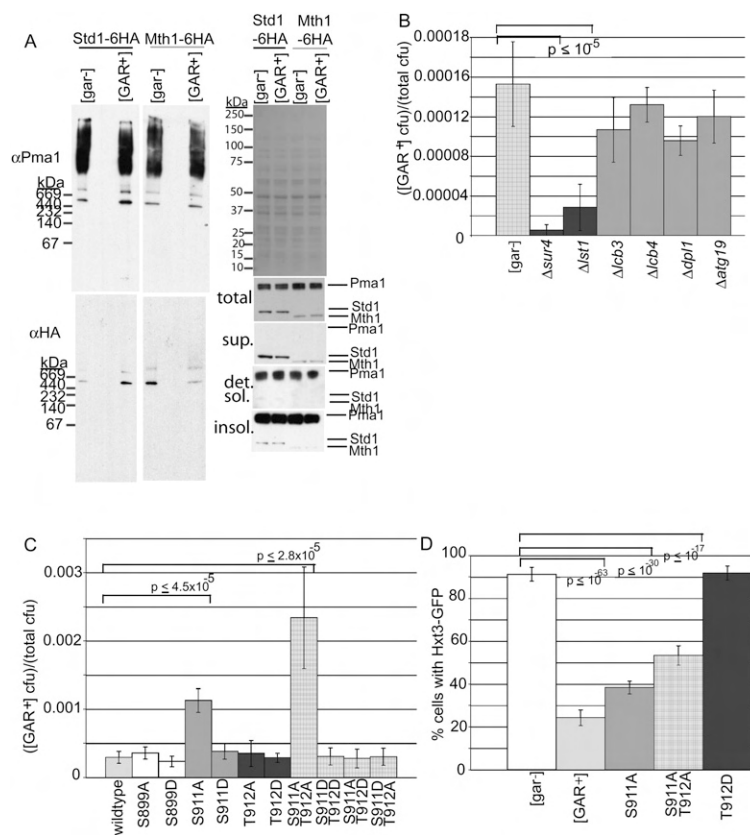


Figure 3. Pma1 is involved in $[GAR^+]$. (A) Native gel of Pma1, Std1, and Mth1 in $[gar^-]$ and $[GAR^+]$. Either Std1 (left) or Mth1 (right) was tagged with six tandem HA tags and samples were processed as described below from $[gar^-]$ and $[GAR^+]$ strains of each background. (Bottom right) Total, supernatant (sup.), digitonin soluble (det. sol.), and digitonin-insoluble (insol.) fractions were run on SDS gels and probed for Pma1 and Std1 or Mth1 as a fractionation control. No differences in Pma1, Std1, or Mth1 levels or localization were detected between $[gar^-]$ and $[GAR^+]$. (Top right) Blots of the total fraction were stained with Ponceau Red to confirm equal amounts of starting material. (B) Measurement of $[GAR^+]$ frequency in knockout mutants of genes previously shown to affect ($\Delta sur4$, $\Delta lst1$) (Roberg et al. 1999; Eisenkolb et al. 2002) or not affect ($\Delta lcb3$, $\Delta lcb4$, $\Delta dpl1$, $\Delta atg19$) (Gaigg et al. 2005; Mazon et al. 2007) attributes of wild-type Pma1. Graph represents the mean \pm standard deviation ($n = 6$). (C) Mutants in phosphorylation sites at the C terminus of Pma1 affect $[GAR^+]$ frequency. Starting strain is haploid, $[gar^-]$, genotype *pma1::kanMX* with p316-PMA1. p314-PMA1 carrying wild-type *PMA1* or mutants of interest were transformed into the starting strain and then p316-PMA1 plasmid selected against by growth on 5-FOA. Graph represents the mean \pm standard deviation ($n = 6$). *P*-values are the binomial distribution of the mean. (D) Pma1 mutants that increase $[GAR^+]$ frequency show decreased levels of Hxt3-GFP. Graph represents the mean \pm standard deviation ($n \geq 6$) and *P*-values were determined using the χ^2 test. Strain background is a hybrid of W303 and S288C.

We explored the relationship between Pma1, [GAR⁺], and the Rgt2/Snf3 glucose signaling pathway. Carbon sources regulate Pma1's phosphorylation state (Lecchi et al. 2005), its ATPase activity (Serrano 1983), and its conformation (Miranda et al. 2002) through residues S899, S911, and T912 in the C-terminal tail, which faces the cytosol (Eraso et al. 2006; Lecchi et al. 2007). We mutated S899, S911, and T912 to alanine, which cannot be phosphorylated, or to aspartic acid, which mimics constitutive phosphorylation. (Phosphorylated S911 and T912 are commonly observed in glucose media and the nonphosphorylated forms when cells are starved of glucose [Lecchi et al. 2007].) S899 mutations and S911D and/or T912D mutations had no effect on [GAR⁺] frequency. However, S911A and S911A/T912A increased the frequency of [GAR⁺] appearance by several-fold (Fig. 3C). Notably, these same mutants also reduced levels of an Hxt3-GFP reporter, both a readout for the Rgt2/Snf3 pathway and the only change in gene expression detected in [GAR⁺] cells (Fig. 3D). These results indicate that Pma1 affects glucose signaling to regulate *HXT3*. In any case, the fact that such subtle mutations in the Pma1 protein affect [GAR⁺] induction confirms that Pma1 plays a key role in [GAR⁺] biology.

The unstructured N terminus of Pma1 is involved in [GAR⁺] propagation

A characteristic of prions is that transient overexpression is sufficient for induction. However, Pma1 is the most abundant plasma membrane protein in yeast (Morsomme et al. 2000), and overexpression is not well tolerated (Eraso et al. 1987). We found that we could obtain a threefold increase in Pma1 protein levels with a *CEN* plasmid and a *GPD* promoter. This caused a corresponding increase in [GAR⁺] frequency (Fig. 4A). Introducing

stop codons at amino acid positions 23 or 59 eliminated this effect (Supplemental Fig. S10). Thus, it is not the nucleic acid sequence but the Pma1 protein that contributes to [GAR⁺] induction. Finally, when the inducing *GPD PMA1* plasmid was lost, the cells remained [GAR⁺]. Thus, a transient increase in *PMA1* was sufficient to induce a heritable change in phenotype.

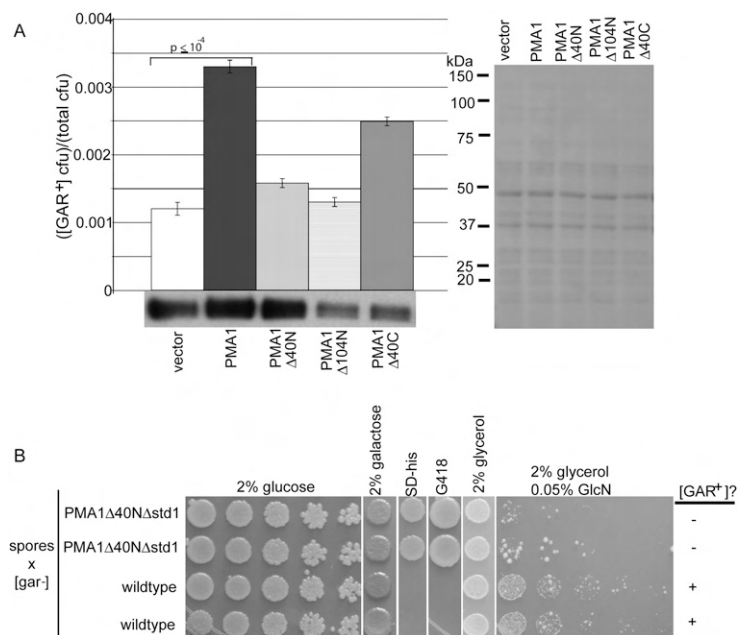
Pma1's N and C termini face the cytosol. The C terminus is predicted to be α -helical and the N terminus unstructured (Morsomme et al. 2000), the latter a characteristic of prions. An N-terminally truncated (Δ 40) mutant of *PMA1* did not increase [GAR⁺] appearance, although the protein was expressed at wild-type levels (Fig. 4A). A C-terminally truncated *PMA1* did increase [GAR⁺] induction, even though its levels were reduced.

[GAR⁺] could be propagated through cells whose only source of Pma1 was a *GAL1*-regulated N-terminal deletion, *PMA1* Δ 40N (Supplemental Fig. S11). Strikingly, however, it did not propagate through a double mutant of *PMA1* Δ 40N and *Std1*, and it did not reappear when wild-type *PMA1* and *STD1* function were restored with crosses (Fig. 4B). (The few glucosamine-resistant colonies that remained were not [GAR⁺] but contained conventional recessive; data not shown.) Thus, once [GAR⁺] has been established, it is maintained in the absence of either *Std1* or the N terminus of Pma1, but not in the absence of both.

[GAR⁺] is sensitive to a Pma1-dependent 'species barrier'

Previously described yeast prion proteins exhibit changes in localization and solubility in the prion state (Uptain and Lindquist 2002) and affect the induction of other prions by cross-templating (Derkatch et al. 2000, 2001). There was no difference in localization of Pma1 or *Std1* between [*gar*⁻] and [GAR⁺] (Supplemental Fig. S12).

Figure 4. Alterations to Pma1 affect [GAR⁺]. (A) [GAR⁺] induction by transient overexpression of *PMA1* in a wild-type background. Data are shown as the mean of [GAR⁺] frequency \pm standard deviation ($n = 6$). Western is total protein probed with α Pma1 antibody and quantified using Scion Image. (Right) The blot was stained with Ponceau Red to confirm equal loading. (B) Propagation of [GAR⁺] is impaired in *PMA1* Δ 40N *Std1* double mutants. Tetrad spores from a [GAR⁺] diploid with the genotype *GAL-PMA1* Δ 40N/*PMA1 std1::kanMX/STD1* were crossed to a [*gar*⁻] strain with wild-type *PMA1* and *STD1* alleles. *PMA1* Δ 40N *Std1* spores cannot propagate [GAR⁺] to wild-type [*gar*⁻] yeast. The few glucosamine-resistant colonies found in the *PMA1* Δ 40N *Std1* background exhibit standard, Mendelian inheritance of the glucosamine resistance phenotype and thus do not carry the [GAR⁺] element.



Neither formed a detectable SDS-resistant species in $[GAR^+]$ (Supplemental Fig. S13). Furthermore, the frequency of $[GAR^+]$ appearance did not change in backgrounds carrying $[PSI^+]$, $[RNQ^+]$, or $[URE3]$, prions that broadly affect the appearance of amyloid-based prions (Supplemental Fig. S14). Analysis of protein extracts by two-dimensional (2D) gel electrophoresis did not reveal any proteins that changed solubility between $[gar^-]$ and $[GAR^+]$ (Supplemental Fig. S15). $[GAR^+]$ was not affected by Hsp104 expression (Fig. 1E). Whatever the manner by which Pma1 and Std1 contribute to the prion state, it is not likely by forming amyloid.

The extremely stable nature of amyloids allows them to be confirmed as prion determinants by “protein only” transformation (Maddelein et al. 2002; Tanaka et al. 2004). The lack of an identifiable amyloid in $[GAR^+]$ cells precluded the use of this procedure for $[GAR^+]$. Instead, to rigorously test the relation between Pma1, Std1, and $[GAR^+]$, we performed a classic “transmission barrier” experiment. Small differences in amino acid sequence cause prions that originate in one species to fail in transmission to another (Santoso et al. 2000; Bagriantsev and Liebman 2004; Chen et al. 2007). If Pma1 and Std1 contribute to a transmission barrier for $[GAR^+]$, it would establish that they are integral to the propagating element.

We chose to study a possible $[GAR^+]$ transmission barrier using *Saccharomyces bayanus* and *Saccharomyces paradoxus*, two closely related sensu stricto species that also exhibit glucose-mediated repression of the utilization of other carbon sources. First, we asked whether diploids of these species could also acquire the ability to use glycerol in the presence of glucosamine (Fig. 5A). They could, and they did so at a higher frequency

than expected for mutation. Indeed, $[GAR^+]$ appeared in *S. bayanus* at an astonishingly high rate (greater than one in 1000 cells). Moreover, the $[GAR^+]$ phenotype was very stable in these cells. Thus, the ability to heritably switch carbon utilization strategies through this prion is broadly used.

We asked whether the Pma1 proteins from *S. bayanus* and *S. paradoxus* can propagate $[GAR^+]$ in *S. cerevisiae*. Sequence differences between the species are slight (Supplemental Fig. S16): *S. bayanus* Pma1 and *S. paradoxus* Pma1 are 96% and 99% identical to *S. cerevisiae* Pma1, respectively. Most of these changes are in the N-terminal region, which is required for prion induction

First, we transformed *S. bayanus* or *S. paradoxus* PMA1 plasmids into an *S. cerevisiae* strain in which a deletion of the essential PMA1 gene was covered by a plasmid encoding *S. cerevisiae* Pma1. The *S. cerevisiae* PMA1 plasmid was then selected against. All cells grew at the same rate on glucose, indicating that the Pma1 protein from these species was fully functional in *S. cerevisiae*. However, when $[GAR^+]$ cells were selected by plating these cells to glycerol–glucosamine medium, the resultant phenotypes were weak, unstable, and appeared at a low frequency. When putative $[GAR^+]$ cells were passaged on nonselective medium and then plated back onto glucosamine-containing medium, many fewer cells with *S. bayanus* or *S. paradoxus* PMA1 maintained the resistant phenotype than cells with *S. cerevisiae* PMA1 (data not shown). Thus, in a background where the entire genome otherwise remains the same, changing the species of origin for Pma1 had a critical effect on $[GAR^+]$ induction and propagation.

Next, we asked whether the *S. bayanus* or *S. paradoxus* Pma1 proteins could propagate a $[GAR^+]$ state received

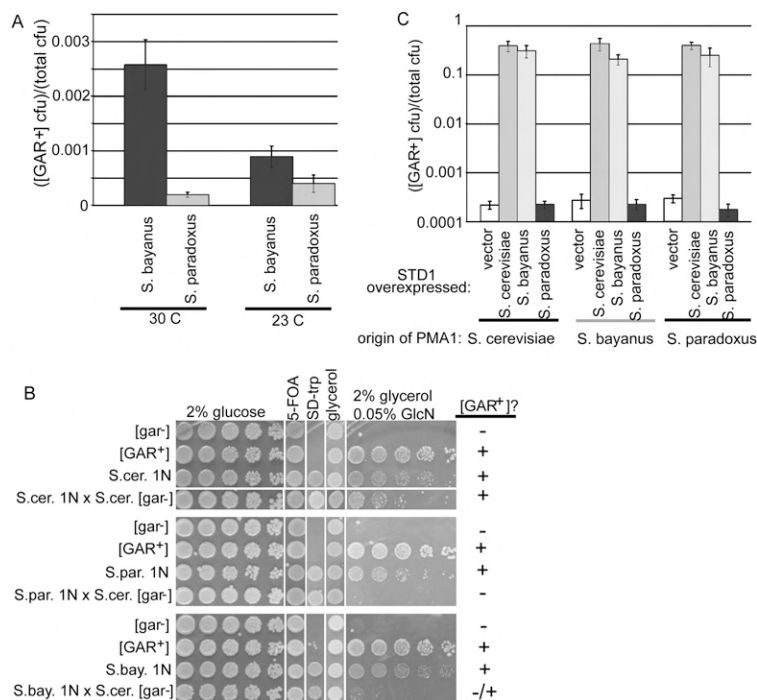


Figure 5. $[GAR^+]$ exhibits a Pma1-dependent species barrier. (A) $[GAR^+]$ frequency of *S. bayanus* and *S. paradoxus* cells grown at 30°C (left), the optimal growth temperature of *S. paradoxus*, or 23°C (right), the optimal growth temperature of *S. bayanus*. Data are shown as the mean of $[GAR^+]$ frequency \pm standard deviation ($n = 6$). (B) Substitution of PMA1 from *S. cerevisiae* with PMA1 from *S. bayanus* or *S. paradoxus* prevents $[GAR^+]$ propagation. Starting strain is haploid, $[GAR^+]$, genotype *pma1::kanMX* with p316-PMA1 *S. cerevisiae* as a covering plasmid. p314-PMA1 carrying PMA1 from *S. cerevisiae* (*S.c.*, top), *S. paradoxus* (*S.par.*, middle), or *S. bayanus* (*S.bay.*, bottom) was transformed into the starting strain and p316-PMA1 *S.c.* selected against by replica plating to 5-FOA (*S.c.* 1N, *S.p.* 1N, or *S.b.* 1N). These haploids were mated to a wild-type *S. cerevisiae* $[gar^-]$ background, restreaked twice, and tested for $[GAR^+]$. Representative data from three independent experiments are shown.

from the *S. cerevisiae* protein. We performed another plasmid shuffle, this time starting with cells already carrying a strong *S. cerevisiae* [GAR⁺] element. We selected against the plasmid carrying the *S. cerevisiae* PMA1 after ~25 generations. After another 25 generations, cells were tested for the ability to grow on glycerol in the presence of glucosamine. Most retained a strong [GAR⁺] phenotype. Thus, strains with *S. bayanus* and *S. paradoxus* PMA1 were capable of accepting and propagating [GAR⁺] from strains with *S. cerevisiae* PMA1 (Fig. 5B), at least after coexpression of both proteins for 25 generations.

Finally, we tested how efficiently [GAR⁺] elements from cells expressing *S. bayanus* or *S. paradoxus* PMA1 could be transmitted back to cells expressing only *S. cerevisiae* PMA1. Multiple [GAR⁺] strains carrying the three PMA1 genes were mated to wild-type [*gar*⁻] cells. Cells expressing PMA1 from *S. paradoxus* could not transmit [GAR⁺] at all, and cells expressing PMA1 from *S. bayanus* transmitted it very inefficiently. Controls expressing *S. cerevisiae* PMA1 transmitted [GAR⁺] efficiently (Fig. 5B). Thus, the PMA1 species of origin creates a strong transmission barrier for [GAR⁺] propagation.

Might Std1, the [GAR⁺] induction factor that is complexed with Pma1 in [GAR⁺] cells, create an induction barrier? Std1 is 81% identical between *S. cerevisiae* and *S. bayanus* but much more divergent in *S. paradoxus* (Supplemental Fig. S17). We transiently overexpressed *STD1* from each organism in [*gar*⁻] *S. cerevisiae* cells carrying each of the three Pma1 genes. *STD1* alleles of *S. cerevisiae* and *S. bayanus* acted as general inducers. They increased the appearance of [GAR⁺] ~1000-fold in strains producing the Pma1 protein of any of the three species (Fig. 5C). In contrast, *S. paradoxus* *STD1* did not induce [GAR⁺] in any. Presumably, some other factor contributes to [GAR⁺] induction in *S. paradoxus*. Most importantly, however, this experiment demonstrates that Std1 creates a strong species barrier for [GAR⁺] induction, confirming its intimate involvement in the prion.

Discussion

The ability of cells to sense and adapt to nutrients is crucial to survival in highly competitive and rapidly fluctuating environments. Here, we describe a cytoplasmically inherited element, [GAR⁺], that is involved in the fundamental processes of glucose sensing and signaling and carbon source utilization. [GAR⁺] arises spontaneously in every *S. cerevisiae* strain tested, as well as sibling species separated by ~5 million years of evolution (Kellis et al. 2004)—*S. paradoxus* and *S. bayanus*—at frequencies much higher than genetic mutations.

[GAR⁺] fulfills all of the genetic criteria established for prions: It is dominant (or at least semidominant). It exhibits non-Mendelian inheritance. It can be transferred via cytoplasmic exchange. Transient changes in the levels of chaperone proteins are sufficient to heritably cure cells of the [GAR⁺] state. Transient changes in the expression of proteinaceous determinants heritably induce [GAR⁺]. The non-Mendelian mechanism of inheritance that best describes [GAR⁺] is that of a prion.

In other ways, however, [GAR⁺] seems very different from previously described yeast prions. It has at least two components: the plasma membrane proton pump Pma1, and the glucose signaling factor Std1. Transient overexpression of either PMA1 or *STD1* is sufficient to establish a heritable conversion to [GAR⁺], yet once [GAR⁺] is established, either is sufficient for propagation. Cells lacking *std1* and also carrying a small deletion in the N terminus of Pma1 cannot propagate [GAR⁺] at all. Pma1 and Std1 associate in an oligomeric complex in [GAR⁺] cells, but this complex is barely detectable in [*gar*⁻] cells. The integral relationship between these proteins and the [GAR⁺] state was tested and confirmed by transmission barrier experiments. Substituting the PMA1 gene from *S. bayanus* or *S. paradoxus* for that of *S. cerevisiae* blocked propagation of [GAR⁺] to *S. cerevisiae* Pma1. Substituting Std1 from *S. paradoxus* eliminated its potency in [GAR⁺] induction.

What, then, is the nature of [GAR⁺]? It does not involve a detectable amyloid form, at least of the Pma1 or Std1 proteins. It also is not sensitive to overexpression or deletion of the general amyloid remodeling protein Hsp104. Hsp104 severs amyloid filaments to ensure orderly inheritance of prion templates to daughter cells. It is required for the propagation of all known prions as well as for 18 of 19 recently discovered prion candidates (Chernoff et al. 1995; Patino et al. 1996; Derkatch et al. 1997; Ness et al. 2002; Cox et al. 2003; Kryndushkin et al. 2003; Shorter and Lindquist 2004, 2006; Jones and Tuite 2005; Tipton et al. 2008; Alberti et al. 2009). Thus, the absence of dependence on Hsp104 makes it rather unlikely that [GAR⁺] involves any amyloid-based element.

One possibility is that [GAR⁺] inheritance and propagation result from heritable alterations in Rgt2/Snf3 signaling involving a self-sustaining feedback loop. Indeed, Std1 and its paralog, Mth1, are subject to many feedback mechanisms involving their own transcription and degradation (Lakshmanan et al. 2003; Moriya and Johnston 2004; Polish et al. 2005; Kim et al. 2006), and Std1 is found both in the nucleus and on the plasma membrane (Schmidt et al. 1999). Furthermore, Pma1 is very abundant and Std1 is extremely scarce (Morsomme et al. 2000). Our data suggest that only a small fraction of Pma1 contributes to [GAR⁺] and that Std1 is the limiting factor. This would be consistent with altered signaling, as only small amounts of the Std1 protein would be necessary to shift the activity of a fraction of Pma1. However, if [GAR⁺] is simply due to altered signaling, the mechanism that maintains it must be remarkably robust, as it has been maintained in a highly stable state in some of our strains for 6 years now, with repeated dilutions into log phase, storage in the freezer and refrigeration, transitions back to room temperature, and growth in liquid and on plates, in a wide variety of different media, through repeated rounds of growth into stationary phase (wherein most aspects of carbon metabolism undergo profound changes), and through starvation-induced meiosis.

Another possibility is that [GAR⁺] starts with a change in the association of Std1 and Pma1 that induces a conformational change in oligomeric species of each. These

can then be maintained in the absence of either Std1 or the Pma1 N terminus, but not in the absence of both (Fig. 6). We do not exclude the possibility that another protein contributes to the $[GAR^+]$ state. Indeed, our observations that *S. paradoxus* acquires $[GAR^+]$ at a high frequency, but that the Pma1 and Std1 proteins of *S. paradoxus* do not reconstitute $[GAR^+]$ in *S. cerevisiae*, suggesting the involvement of another protein. (This protein might even form amyloid, but if so it does not require Hsp104 and has escaped detection in our genetic screens.)

Of course, models involving self-perpetuating signaling loops and conformational changes are not mutually exclusive. Associations between Pma1 and Std1 might result in a conformational change that alters signaling and sets up a robust feedback loop that helps maintain the association, either between those same molecules of Pma1 and Std1 or between other molecules and these proteins (Fig. 6). It will be of great interest to determine what might render such states stable enough to be so robustly heritable.

Another remaining question is the precise reason why cells carrying $[GAR^+]$ are able to grow on glycerol in the presence of glucosamine. We hypothesize that the $[GAR^+]$ phenotype involves altered signaling through a glucose-sensing pathway, likely through Std1's previously reported ability to interact with the DNA-binding protein Rgt1 (Fig. 6; Lakshmanan et al. 2003). Experiments investigating gene expression patterns over a much broader range of carbon sources and time points than examined here, as well as chromatin immunoprecipitation experiments with Std1 and Rgt1, may prove illuminating.

Whatever the mechanism may prove to be, Pma1, the major plasma membrane ATPase, and Std1, a much rarer and poorly understood signaling protein, contribute to a prion-like phenotypic state that heritably alters fundamental decisions about carbon source utilization. This heritable element, $[GAR^+]$, has all of the definitive characteristics of a prion. It has been stated that prion-mediated epigenetic states are simply diseases of yeast (Nakayashiki et al. 2005). Our findings that such an element controls something as fundamental to yeast biology as glucose repression, and that this element spontaneously arises at high frequency in diverse strains and sibling species, suggests that such epigenetic switches are actually integral to yeast biology. Clearly, self-propagating protein-based elements (prions) that can stably perpetuate biological states across generations operate over a much broader mechanistic landscape than supposed previously.

Materials and methods

Yeast strains and genetic manipulations

Strain construction and manipulation followed standard yeast techniques. A list of strains and plasmids used in this study is available in Supplemental Tables S1 and S2. Unless otherwise stated, data shown are from genetic background W303. Fivefold dilutions were used for all spotting assays. Media used were yeast peptone-based medium containing the designated carbon source (YPD, YPglycerol, and YPgalactose), synthetic medium lacking a particular amino acid (SD), or glycerol glucosamine medium (GGM; 1% yeast extract, 2% peptone, 2% glycerol, 0.05% D-[+]-glucosamine [Sigma G4875]).

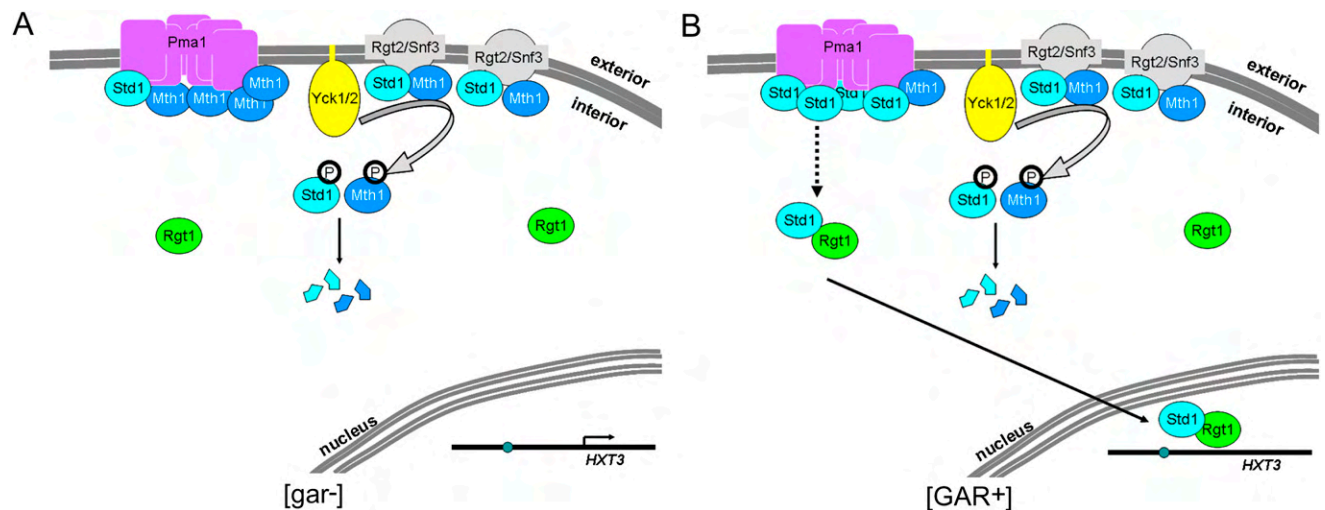


Figure 6. Pma1 and the Rgt2/Snf3 glucose signaling pathway We propose that Pma1 acts as a part of the Rgt2/Snf3 signaling pathway. (A) In $[gar^-]$ glucose-grown cells, Pma1 associates with Mth1. The glucose signal is propagated through Snf3 and Rgt2 to Yck1 and Yck2, which phosphorylate Mth1 and Std1. This phosphorylation marks Mth1 and Std1 for degradation, leaving their interacting partner, Rgt1, free in the cytosol, where it does not repress transcription at the *HXT3* locus. (B) Under $[GAR^+]$ conditions, *HXT3* transcription is repressed, which resembles that of cells grown in a carbon source other than glucose. Pma1 associates with Std1, which somehow facilitates the repression of *HXT3*, possibly by altering the affinity of Std1 for Rgt1. Association with Std1 has been shown previously to facilitate the binding of Rgt1 to DNA (Lakshmanan et al. 2003). The association between Pma1 can either be transient or stable, but either way it aids in the establishment of an altered signaling pathway. This altered pathway is then maintained either by the contained association between Std1 and Pma1 or by a feedback loop within the signaling cascade itself.

Brown and Lindquist

[GAR⁺] frequency assays and isolation of [GAR⁺]

Cultures for [GAR⁺] frequency assays were grown overnight in 2% glucose, either YPD or SD, subcultured in the same, then grown to early exponential phase (OD₆₀₀ = 0.2–0.4). Cultures were plated straight to GGM and diluted 10⁻⁴ for plating to YPD. To isolate [GAR⁺] for further study, colonies from GGM were restreaked once to GGM then used in downstream applications. Unless otherwise stated, error bars in [GAR⁺] frequency assays represent the standard deviation and *P*-values are the binomial distribution of the mean. In all assays for [GAR⁺] propagation, cells were passaged for >100 generations before testing for growth on glycerol in the presence of glucosamine. Sporulation was performed by growing to diauxic shift in YPD or SD, plating to sporulation plates (1% potassium acetate, 0.05% dextrose, 0.1% yeast extract, 0.01% complete amino acid mix [Bio101]), and incubating at 23°C until sporulated.

Genetic, biochemical, and cell biological analysis

Gene expression profiling, Western blotting, immunoprecipitation, fluorescent microscopy, Blue Native gel analysis, protease sensitivity analysis, and genetic screens were all performed using standard procedures. Detailed descriptions are available in the Supplemental Material.

Acknowledgments

We thank and acknowledge Neal Sondheimer, whose initial investigation first suggested that [GAR⁺] might be a prion-based phenotype (Sondheimer 2000). We thank Amy Chang for gifts of an antibody and strains, and general advice on working with Pma1; Tom Rapaport for a Sec61 antibody; and Eric Spooner for mass spectrometry. Whitehead Institute Center for Microarray Technology performed cDNA synthesis, labeling, and hybridization reactions for the microarrays. We thank members of the Lindquist laboratory for providing comments and advice. This work was supported by the Mathers Foundation (to S.L.), DuPont MIT Alliance (to S.L.) and NIH grant GM25874. J.C.S.B is supported by an NSF Graduate Research Fellowship and the Arthur Siegel Fellowship from Whitehead Institute for Biomedical Research.

References

- Aguzzi A, Heikenwalder M, Polymenidou M. 2007. Insights into prion strains and neurotoxicity. *Nat Rev Mol Cell Biol* **8**: 552–561.
- Alberti S, Halfmann R, King O, Kapila A, Lindquist S. 2009. A systematic survey identifies prions and illuminates sequence features of prionogenic proteins. *Cell* **137**: 146–158.
- Bagriantsev S, Liebman SW. 2004. Specificity of prion assembly in vivo: [PSI⁺] AND [PIN⁺] form separate structures in yeast. *J Biol Chem* **279**: 51042–51048.
- Ball AJS, Wong DK, Elliott JJ. 1976. Glucosamine resistance in yeast. I. A preliminary genetic analysis. *Genetics* **84**: 311–317.
- Brachmann A, Baxa U, Wickham RB. 2005. Prion generation *in vitro*: Amyloid of Ure2p is infectious. *EMBO J* **24**: 3082–3092.
- Chen B, Newnam GP, Chernoff YO. 2007. Prion species barrier between the closely related yeast proteins is detected despite coaggregation. *Proc Natl Acad Sci* **104**: 2791–2796.
- Chernoff YO, Derkach IL, Inge-Vechtormov SG. 1993. Multicopy SUP35 gene induces de-novo appearance of psi-like factors in the yeast *Saccharomyces cerevisiae*. *Curr Genet* **24**: 268–270.
- Chernoff YO, Lindquist SL, Ono B, Inge-Vechtormov SG, Liebman SW. 1995. Role of the chaperone protein Hsp104 in propagation of the yeast prion-like factor [psi⁺]. *Science* **268**: 880–884.
- Chien P, Weissman JS, DePace AH. 2004. Emerging principles of conformation-based prion inheritance. *Annu Rev Biochem* **73**: 617–656.
- Conde J, Fink GR. 1976. A mutant of *Saccharomyces cerevisiae* defective for nuclear fusion. *Proc Natl Acad Sci* **73**: 3651–3655.
- Courchesne WE, Magasanik B. 1988. Regulation of nitrogen assimilation in *Saccharomyces cerevisiae*: Roles of the URE2 and GLN3 genes. *J Bacteriol* **170**: 708–713.
- Coustou V, Deleu C, Saupe S, Begueret J. 1997. The protein product of the het-s heterokaryon incompatibility gene of the fungus *Podospora anserina* behaves as a prion analog. *Proc Natl Acad Sci* **94**: 9773–9778.
- Cox BS. 1965. PSI, a cytoplasmic suppressor of the super-suppressor in yeast. *Heredity* **20**: 505–521.
- Cox B, Ness F, Tuite MF. 2003. Analysis of the generation and segregation of propagons: Entities that propagate the [PSI⁺] prion in yeast. *Genetics* **165**: 23–33.
- Derkatch IL, Chernoff YO, Kushnirov VV, Inge-Vechtormov SG, Liebman SW. 1996. Genesis and variability of [PSI⁺] prion factors in *Saccharomyces cerevisiae*. *Genetics* **144**: 1375–1386.
- Derkatch IL, Bradley ME, Zhou P, Chernoff YO, Liebman SW. 1997. Genetic and environmental factors affecting the de novo appearance of the [PSI⁺] prion in *Saccharomyces cerevisiae*. *Genetics* **147**: 507–519.
- Derkatch IL, Bradley ME, Masse SV, Zadorsky SP, Polozkov GV, Inge-Vechtormov SG, Liebman SW. 2000. Dependence and independence of [PSI⁺] and [PIN⁺]: A two-prion system in yeast? *EMBO J* **19**: 1942–1952.
- Derkatch IL, Bradley ME, Hong JY, Liebman SW. 2001. Prions affect the appearance of other prions: The story of [PIN⁺]. *Cell* **106**: 171–182.
- Du Z, Park K-W, Yu H, Fan Q, Li L. 2008. Newly identified prion linked to the chromatin-remodeling factor Swi1 in *Saccharomyces cerevisiae*. *Nat Genet* **40**: 460–465.
- Eisenkolb M, Zenzmaier C, Leitner E, Schneider R. 2002. A specific structural requirement for ergosterol in long-chain fatty acid synthesis mutants important for maintaining raft domains in yeast. *Mol Biol Cell* **13**: 4414–4428.
- Eraso P, Cid A, Serrano R. 1987. Tight control of the amount of yeast plasma membrane ATPase during changes in growth conditions and gene dosage. *FEBS Lett* **224**: 193–197.
- Eraso P, Mazón MJ, Portillo F. 2006. Yeast protein kinase Ptk2 localizes at the plasma membrane and phosphorylates in vitro the C-terminal peptide of the H⁺-ATPase. *Biochim Biophys Acta* **1758**: 164–170.
- Ferreira PC, Ness F, Edwards SR, Cox BS, Tuite MF. 2001. The elimination of the yeast [PSI⁺] prion by guanidine hydrochloride is the result of Hsp104 inactivation. *Mol Microbiol* **40**: 1357–1369.
- Gaigg B, Timischl B, Corbino L, Schneider R. 2005. Synthesis of sphingolipids with very long chain fatty acids but not ergosterol is required for routing of newly synthesized plasma membrane ATPase to the cell surface of yeast. *J Biol Chem* **280**: 22515–22522.
- Giaever G, Chu AM, Ni L, Connelly C, Riles L, Veronneau S, Dow S, Lucau-Danila A, Anderson K, Andre B, et al. 2002. Functional profiling of the *Saccharomyces cerevisiae* genome. *Nature* **418**: 387–391.
- Glover JR, Kowal AS, Schirmer EC, Patino MM, Liu J-J, Lindquist S. 1997. Self-seeded fibers formed by Sup35, the protein determinant of [PSI⁺], a heritable prion-like factor of *S. cerevisiae*. *Cell* **89**: 811–819.

- Hockney RC, Freeman RF. 1980. Gratuitous catabolite repression by glucosamine of maltose utilization in *Saccharomyces cerevisiae*. *J Gen Microbiol* **121**: 469–474.
- Jones GW, Tuite MF. 2005. Chaperoning prions: The cellular machinery for propagating an infectious protein? *Bioessays* **27**: 823–832.
- Jung G, Masison DC. 2001. Guanidine hydrochloride inhibits Hsp104 activity in vivo: A possible explanation for its effect in curing yeast prions. *Curr Microbiol* **43**: 7–10.
- Kellis M, Birren BW, Lander ES. 2004. Proof and evolutionary analysis of ancient genome duplication in the yeast *Saccharomyces cerevisiae*. *Nature* **428**: 617–624.
- Kim J-H, Polish J, Johnston M. 2003. Specificity and regulation of DNA binding by the yeast glucose transporter gene repressor Rgt1. *Mol Cell Biol* **23**: 5208–5216.
- Kim JH, Brachet V, Moriya H, Johnston M. 2006. Integration of transcriptional and posttranslational regulation in a glucose signal transduction pathway in *Saccharomyces cerevisiae*. *Eukaryot Cell* **5**: 167–173.
- King C-Y, Diaz-Avalos R. 2004. Protein-only transmission of three yeast prion strains. *Nature* **428**: 319–323.
- Kryndushkin DS, Alexandrov IM, Ter-Avanesyan MD, Kushnirov VV. 2003. Yeast [PSI⁺] prion aggregates are formed by small Sup35 polymers fragmented by Hsp104. *J Biol Chem* **278**: 49636–49643.
- Kunz BA, Ball AJ. 1977. Glucosamine resistance in yeast II: Cytoplasmic determinants conferring resistance. *Mol Gen Genet* **153**: 169–177.
- Lacroute F. 1971. Non-mendelian mutation allowing ureidosuccinic acid uptake in yeast. *J Bacteriol* **106**: 519–522.
- Lakshmanan J, Mosley A, Özcan S. 2003. Repression of transcription by Rgt1 in the absence of glucose requires Std1 and Mth1. *Curr Genet* **44**: 19–25.
- Lecchi S, Allen KE, Pardo JP, Mason AB, Slayman CW. 2005. Conformational changes of yeast plasma membrane H⁺(+)-ATPase during activation by glucose: Role of threonine-912 in the carboxy-terminal tail. *Biochem* **44**: 16624–16632.
- Lecchi S, Nelson CJ, Allen KE, Swaney DL, Thompson KL, Coon JJ, Sussman MR, Slayman CW. 2007. Tandem phosphorylation of Ser-911 and Thr-912 at the C terminus of yeast plasma membrane H⁺-ATPase leads to glucose-dependent activation. *J Biol Chem* **282**: 35471–35481.
- Lee MC, Hamamoto S, Schekman R. 2002. Ceramide biosynthesis is required for the formation of the oligomeric H⁺-ATPase Pma1p in the yeast endoplasmic reticulum. *J Biol Chem* **277**: 22395–22401.
- Leonardo B, Aaron R, Gerald M, Joshua L. 2002. The FLEXGene repository: Exploiting the fruits of the genome projects by creating a needed resource to face the challenges of the post-genomic era. *Arch Med Res* **33**: 318–324.
- Maddelein M-L, Dos Reis S, Duvezin-Caubet S, Couлары-Salin B, Saupe SJ. 2002. Amyloid aggregates of the HET-s prion protein are infectious. *Proc Natl Acad Sci* **99**: 7402–7407.
- Masison DC, Wickner RB. 1995. Prion-inducing domain of yeast Ure2p and protease resistance of Ure2p in prion-containing cells. *Science* **270**: 93–95.
- Mazon MJ, Eraso P, Portillo F. 2007. Efficient degradation of misfolded mutant Pma1 by endoplasmic reticulum-associated degradation requires Atg19 and the Cvt/autophagy pathway. *Mol Microbiol* **63**: 1069–1077.
- Miranda M, Pardo JP, Allen KE, Slayman CW. 2002. Stalk segment 5 of the yeast plasma membrane H⁺-ATPase. Labeling with a fluorescent maleimide reveals a conformational change during glucose activation. *J Biol Chem* **277**: 40981–40988.
- Moriya H, Johnston M. 2004. Glucose sensing and signaling in *Saccharomyces cerevisiae* through the Rgt2 glucose sensor and casein kinase I. *Proc Natl Acad Sci* **101**: 1572–1577.
- Moriyama H, Edskes HK, Wickner RB. 2000. [URE3] prion propagation in *Saccharomyces cerevisiae*: Requirement for chaperone Hsp104 and curing by overexpressed chaperone Ydj1p. *Mol Cell Biol* **20**: 8916–8922.
- Morsomme P, Slayman CW, Goffeau A. 2000. Mutagenic study of the structure, function and biogenesis of the yeast plasma membrane H⁺-ATPase. *Biochim Biophys Acta* **1469**: 133–157.
- Nakayashiki T, Kurtzman CP, Edskes HK, Wickner RB. 2005. Yeast prions [URE3] and [PSI⁺] are diseases. *Proc Natl Acad Sci* **102**: 10575–10580.
- Nemecek J, Nakayashiki T, Wickner RB. 2009. A prion of the yeast netacaspase homolog (Mca1p) detected by a genetic screen. *Proc Natl Acad Sci* **106**: 1892–1896.
- Ness F, Ferreira P, Cox BS, Tuite MF. 2002. Guanidine hydrochloride inhibits the generation of prion ‘seeds’ but not prion protein aggregation in yeast. *Mol Cell Biol* **22**: 5593–5605.
- Nevado J, Heredia CF. 1996. Galactose induces in *Saccharomyces cerevisiae* sensitivity of the utilization of hexose to inhibition by D-glucosamine. *Can J Microbiol* **42**: 6–11.
- Ohnishi G, Endo K, Doi A, Fujita A, Daigaku Y, Nunoshiba T, Yamamoto K. 2004. Spontaneous mutagenesis in haploid and diploid *Saccharomyces cerevisiae*. *Biochem Biophys Res Commun* **325**: 928–933.
- Oka M, Kimata Y, Mori K, Kohno K. 1997. *Saccharomyces cerevisiae* KAR2 (BiP) gene expression is induced by loss of cytosolic HSP70/Ssalp through a heat shock element-mediated pathway. *J Biochem* **121**: 578–584.
- Patel BK, Liebman SW. 2007. “Prion-proof” for [PIN⁺]: Infection with in vitro-made amyloid aggregates of Rnq1p(132–405) induces [PIN⁺]. *J Mol Biol* **365**: 773–782.
- Patel BK, Gavin-Smyth J, Liebman SW. 2009. The yeast global transcriptional co-repressor protein Cyc8 can propagate as a prion. *Nat Cell Biol* **11**: 344–349.
- Patino MM, Liu J-J, Glover JR, Lindquist S. 1996. Support for the prion hypothesis for inheritance of a phenotypic trait in yeast. *Science* **273**: 622–626.
- Paushkin SV, Kushnirov VV, Smirnov VN, Ter-Avanesyan MD. 1996. Propagation of the yeast prion-like [psi⁺] determinant is mediated by oligomerization of the SUP35-encoded polypeptide chain release factor. *EMBO J* **15**: 3127–3134.
- Polish JA, Kim J-H, Johnston M. 2005. How the Rgt1 transcription factor of *Saccharomyces cerevisiae* is regulated by glucose. *Genetics* **169**: 583–594.
- Prusiner SB. 1998. Prions. *Proc Natl Acad Sci* **95**: 13363–13383.
- Rizet G. 1952. Les phenomenes de barrage chez *Podospora anserina*: Analyse genetique des barrages entre les souches s et S. *Rev Cytol Biol Veg* **13**: 51–92.
- Roberg KJ, Crotwell M, Espenshade P, Gimeno R, Kaiser CA. 1999. LST1 is a SEC24 homologue used for selective export of the plasma membrane ATPase from the endoplasmic reticulum. *J Cell Biol* **145**: 659–672.
- Santangelo GM. 2006. Glucose signaling in *Saccharomyces cerevisiae*. *Microbiol Mol Biol Rev* **70**: 253–282.
- Santoso A, Chien P, Osheroovich LZ, Weissman JS. 2000. Molecular basis of a yeast prion species barrier. *Cell* **100**: 277–288.
- Schmidt MC, McCartney RR, Zhang X, Tillman TS, Solimeo H, Wolf S, Almonte C, Watkins SC. 1999. Std1 and Mth1 proteins interact with the glucose sensors to control glucose-regulated gene expression in *Saccharomyces cerevisiae*. *Mol Cell Biol* **19**: 4561–4571.
- Serio TR, Cashikar AG, Kowal AS, Sawicki GJ, Moslehi JJ, Serpell L, Arnsdorf ME, Lindquist SL. 2000. Nucleated

Brown and Lindquist

- conformational conversion and the replication of conformational information by a prion determinant. *Science* **289**: 1317–1321.
- Serrano R. 1983. In vivo glucose activation of the yeast plasma membrane ATPase. *FEBS Lett* **156**: 11–14.
- Serrano R, Kielland-Brandt MC, Fink GR. 1986. Yeast plasma membrane ATPase is essential for growth and has homology with (Na⁺ + K⁺), K⁺- and Ca²⁺-ATPases. *Nature* **319**: 689–693.
- Shorter J, Lindquist S. 2004. Hsp104 catalyzes formation and elimination of self-replicating Sup35 prion conformer. *Science* **304**: 1793–1797.
- Shorter J, Lindquist S. 2005. Prions as adaptive conduits of memory and inheritance. *Nat Rev Genet* **6**: 435–450.
- Shorter J, Lindquist S. 2006. Destruction or potentiation of different prions catalyzed by similar Hsp104 remodeling activities. *Mol Cell* **23**: 425–438.
- Sondheimer N. 2000. "The identification of novel prion elements in *Saccharomyces cerevisiae*." PhD thesis, University of Chicago, Chicago.
- Sondheimer N, Lindquist S. 2000. Rnq1: An epigenetic modifier of protein function in yeast. *Mol Cell* **5**: 163–172.
- Stansfield I, Jones KM, Kushnirov VV, Dagkesamanskaya AR, Poznyakovski AI, Paushkin SV, Nierras CR, Cox BS, Ter-Avanesyan MD, Tuite MF. 1995. The products of the SUP45 (eRF1) and SUP35 genes interact to mediate translation termination in *Saccharomyces cerevisiae*. *EMBO J* **14**: 4365–4373.
- Sweeny EA, Shorter J. 2008. Prion proteostasis: Hsp104 meets its supporting cast. *Prion* **2**: 135–140.
- Tanaka M, Chien P, Naber N, Cooke R, Weissman JS. 2004. Conformational variations in an infectious protein determine prion strain differences. *Nature* **428**: 323–328.
- Ter-Avanesyan MD, Kushnirov VV, Dagkesamanskaya AR, Didichenko SA, Chernoff YO, Inge-Vechtomov SG, Smirnov VN. 1993. Deletion analysis of the SUP35 gene of the yeast *Saccharomyces cerevisiae* reveals two non-overlapping functional regions of the encoded protein. *Mol Microbiol* **7**: 683–692.
- Tipton KA, Verges KJ, Weissman JS. 2008. In vivo monitoring of the prion replication cycle reveals a critical role for Sis1 in delivering substrates to Hsp104. *Mol Cell* **32**: 584–591.
- Uptain SM, Lindquist S. 2002. Prions as protein-based genetic elements. *Annu Rev Microbiol* **56**: 703–741.
- Werner-Washburne M, Stone DE, Craig EA. 1987. Complex interactions among members of an essential subfamily of hsp70 genes in *Saccharomyces cerevisiae*. *Mol Cell Biol* **7**: 2568–2577.
- Wickner RB. 1994. [URE3] as an altered URE2 protein: Evidence for a prion analog in *Saccharomyces cerevisiae*. *Science* **264**: 566–569.
- Wickner RB, Edskes HK, Ross ED, Pierce MM, Baxa U, Brachmann A, Shewmaker F. 2004. Prion genetics: New rules for a new kind of gene. *Annu Rev Genet* **38**: 681–707.

Supplementary Materials and Methods

Western blotting

Protein samples were run on 4-12% SDS gels from Invitrogen and blotted to PVDF using standard techniques. All samples to be tested for Pma1 were incubated in loading buffer (4% SDS, 50mM Tris pH 6.8, 2% β -mercaptoethanol, 10% glycerol) for 10min at 37°C prior to loading. Monoclonal α Pma1 mouse antibody was obtained from EnCor Biotechnology. Polyclonal α Pma1 rabbit antibody was a gift from Amy Chang. Polyclonal α Sec61 antibody was a gift from Tom Rapaport. Immune complexes were visualized by ECL.

Gene expression profiling

PolyA RNA was produced using standard methods (Schmitt et al. 1990) from cells grown in 2% glucose that were about to undergo diauxic shift. Samples were labeled and hybridized to Affymetrix S98 arrays by the Whitehead Center for Microarray Technology using standard methods. Data was analyzed using Genespring and TIGR Multiexperiment Viewer. Data was deposited at NCBI GEO (<http://www.ncbi.nlm.nih.gov/geo/query/acc.cgi?acc=GSE12479>).

Hxt3-GFP analysis

Hxt3-GFP signal was observed starting at $OD_{600} = 0.7$ in an S288C background. Microscopy was performed on a Zeiss axioplan using Metamorph software.

Immunoprecipitation

IPs were performed using standard procedures in IP buffer (50mM HEPES pH 7.5, 150mM NaCl, 2.5mM EDTA, 1% V/V Triton X-100, 40mM NEM, 3mM PMSF, 1 Protease Inhibitor Cocktail Tablet per 5ml buffer [Roche]). Cells were lysed either by bead beating (9 x 30sec with 15sec on ice between) or spheroplasting (30min at 30°C in 1M D-sorbitol, 0.1M EDTA, 0.5mg/ml zymolase) with comparable results. Lysates were adjusted for protein concentration, incubated with protein G agarose beads (Roche) for 30min at 4°C, centrifuged at 3300 x g for 2min, and the supernatant collected. The supernatant was then incubated with 10µg mouse αHA antibody (Sigma) for 1 hour at 4°C followed by incubation with 50µl protein G beads (Roche) for 1 hour at 4°C. Samples then washed six times in chilled IP buffer, boiled to elute, and run on a 4-12% SDS gel. Gels were either stained with colloidal Coomassie (Invitrogen) or blotted for Pma1. Std1- and Mth1-tagged strains were shown to acquire and stably maintain the [*GAR*⁺] element (data not shown).

Blue Native gels

Midlog cultures (150ml, OD₆₀₀~0.5) were lysed by bead beating (9 x 30sec with 15sec on ice between) into sorbitol buffer (250mM sorbitol, 50mM Tris pH 7.5, 3mM PMSF, 1 Protease Inhibitor Cocktail Tablet per 5ml buffer [Roche]). Samples were equalized at a concentration of 15µg/µl in 650µl, a “total” cellular protein sample collected, and centrifuged at 16000 x g for 30min at 4°C. The supernatant was removed, a sample saved for downstream analysis, and the pellet washed once in sorbitol buffer. The pellet was resuspended in sorbitol buffer (200µl), and an aliquot (95µl) incubated 20min on ice with

digitonin to 1% (Calbiochem). These samples were then centrifuged at 16000 x g at 4°C for 30min and separated into supernatant (“digitonin soluble”) and pellet (“digitonin insoluble”) fractions. 15µl of the soluble fraction was incubated with Coomassie G-250 at a detergent to dye ratio of 8:1 for 10min on ice then loaded onto 3-12% Blue Native gel (Invitrogen) and run at 4°C as per the manufacturer’s instructions.

Trypsin digestion

Cells were grown to mid exponential phase (OD₆₀₀~0.5), washed three times in water, then lysed by bead beating (9 x 30sec with 15sec on ice between) into sorbitol buffer (250mM sorbitol, 50mM Tris pH 7.5, 3mM PMSF, 1 Protease Inhibitor Cocktail Tablet per 5ml buffer [Roche]). Samples were centrifuged at 16000 x g for 30min at 4°C, the supernatant removed, then washed three times in sorbitol buffer with protease inhibitors and three times in sorbitol buffer without protease inhibitors. For trypsin reactions, 10µg protein and 4µg trypsin (Worthington) were used in a total volume of 20µl. Reactions were incubated at 30°C and stopped after the designated point in time by addition of 2µl soybean trypsin inhibitor (10mg/ml stock, from Sigma) then immediately frozen in an ethanol/dry ice bath. Samples were run on gels as described above, probed with monoclonal αPma1, stripped, and re-probed with polyclonal αSec61.

Screen of S. cerevisiae deletion library for [GAR⁺] induction-deficient knockout mutants

Library plates were inoculated into 96-well plates containing 200µl YPD and grown 48 hours at 30°C. Cells were then resuspended and plated to media containing 2% glucose, 2% glycerol, or 2% glycerol + 0.03% glucosamine (optimal concentration for the BY

strain background). Plates were photographed every 24 hours for seven days. Wild-type controls showed the appearance of glucosamine-resistant colonies after five days. Mutants that exhibited earlier appearance of glucosamine-resistant colonies were either completely resistant to glucosamine (when every cell in the population grew on glucosamine medium) or exhibited high rates of appearance of [*GAR*⁺] (when a subset of the population grew on glucosamine medium). Mutants that showed few or no glucosamine-resistant colonies after seven days were considered deficient in induction or maintenance of [*GAR*⁺]. Knockout mutants that exhibited a growth defect on glucose- or glycerol-based media were excluded from the analysis. Data were obtained from two replicates of two independent experiments.

*Screen for ORFs that induce [*GAR*⁺] following transient overexpression*

A library of plasmids, each containing a single *S. cerevisiae* ORF under control of the inducible *GALI* promoter, was mated to a strain containing a *GAL*-estradiol fusion plasmid (Quintero et al. 2007). The latter allows induction of *GALI* promoters by growth on estradiol without galactose. We selected for diploids carrying both plasmids on glucose medium lacking histidine (estradiol plasmid marker) and uracil (*GALI* plasmid marker). Following this selection, cells were grown in selective medium containing 1mM estradiol, which induces gene expression (Quintero et al. 2007), for 24 hours. These cells were harvested, washed once in H₂O, resuspended in H₂O, and spotted to media containing either 2% glucose or 2% glycerol + 0.05% glucosamine. Plates were imaged every 24 hours for seven days. Control spots containing cells carrying the empty induction plasmid exhibited glucosamine-resistant colonies after five days. Data were

collected from two independent screens. Spots that showed growth on glucosamine-medium prior to five days were retested individually.

2D gel electrophoresis

2D gels were performed as previously described (Görg et al. 2004) with the following modifications. Mid-exponential phase yeast cells were lysed by spheroplasting (0.5mg/ml zymolase), resuspending in buffer (50mM HEPES, 150mM NaCl, 2.5mM EDTA, 1%(V/V) TritonX-100, and protease inhibitors) then running through a 21G needle. Protein samples were separated into supernatant and pellet fractions by centrifuging at 14,000g. Samples were diluted in rehydration solution and IPG buffer (GE Healthcare) and 1mg total protein was loaded onto 11cm IPG DryStrip pH 3-11 nonlinear (GE Healthcare). IPG strips were rehydrated overnight then run on a Multiphor II electrophoresis apparatus. The second dimension was run on 4-12% gradient SDS gels from GE Healthcare. Gels were visualized using a Colloidal Blue Straining Kit (Invitrogen).

Indirect Immunofluorescence

Immunofluorescence experiments were performed as previously described (Amberg et al. 2005). Anti-HA antibody (Sigma) was used at 1:100 dilution. Anti-mouse Texas Red (Molecular Probes) was used at 1:100 dilution.

SDS solubility

Protein samples for measuring the SDS solubility of Pma1, Std1, and Sup35 extracted as described in the Native gel protocol in Materials and Methods. Total protein was diluted in loading buffer to a final SDS concentration on 4% then incubated 10min at 37°C or boiled for 5min, as indicated. Transfer to PVDF membrane and Western blotting was as described.

Table S1: Knockout mutants able to grow on glycerol in the absence of glucosamine

ORF number	gene name	ORF number	gene name
YAL056W	GPB2	YIL148W	RPL40A
YBL079W	NUP170	YJL003W	COX16
YCL036W	GFD2	YJL179W	PFD1
YCR044C	PER1	YJR039W	
YCR050C		YJR055W	HIT1
YCR085W		YJR058C	APS2
YDL006W	PTC1	YJR118C	ILM1
YDL160C	DHH1	YKL073W	LHS1
YDL194W	SNF3	YKR024C	DBP7
YDL232W	OST4	YKR055W	RHO4
YDR074W	TPS2	YLR402W	
YDR129C	SAC6	YML048W	GSF2
YDR521W		YML063W	RPS1B
YER115C	SPR6	YML094W	GIM5
YER131W	RPS26B	YML115C	VAN1
YGL015C		YML129C	COX14
YGL084C	GUP1	YMR074C	
YGL127C	SOH1	YMR307W	GAS1
YGL197W	MDS3	YNL133C	FYV6
YGR036C	CAX4	YNL238W	KEX2
YGR071C		YNR052C	POP2
YGR159C	NSR1	YOL081W	IRA2
YGR180C	RNR4	YOR175C	
YGR229C	SMI1	YOR253W	NAT5
YHL019C	APM2	YPL090C	RPS6A
YHL033C	RPL8A	YPL178W	CBC2
YHR075C	PPE1	YPL179W	PPQ1
YHR087W		YPR129W	SCD6
YIL040W	APQ12	YPR170C	
significant GO categories: signal transduction (p = 0.013)			

Table S2: Knockout mutants with a reduced frequency of [*GAR*⁺] appearance

ORF number	gene name	significant GO terms	p-value	genes	
YAL013W	DEP1	organelle organization and biogenesis	0.002	DEP1	
YBL061C	SKT5			MIS1	
YBR084W	MIS1			RPP1A	
YBR120C	CBP6			RTF1	
YDL081C	RPP1A			SUR4	
YDR017C	KCS1			RPL13B	
YGL244W	RTF1			DMA2	
YJL165C	HAL5			CSE2	
YKL038W	RGT1		protein modification process	0.034	DEP1
YLR372W	SUR4				MIS1
YMR142C	RPL13B				RTF1
YNL040W					DMA2
YNL116W	DMA2		translation	0.001	MIS1
YNR010W	CSE2				CBP6
YOL023W	IFM1				RPP1A
YOR333C					RPL13B
YDR277C	MTH1				IFM1
YOR047C	STD1		ligase activity	0.039	MIS1
				DMA2	
		transcription regulator activity	0.005	DEP1	
				RTF1	
				RGT1	
				CSE2	

Table S3: Knockout mutants that switch to [*GAR*⁺] at high frequency

ORF number	gene name	significant GO terms	p-value	genes
YGL028C	SCW11	carbohydrate metabolic processing	0.049	INM1
YGL041C				KRE6
YGL138C		cytokinesis	0.02	SCW11
YGR027C	RPS25A			BUD2
YHR046C	INM1	hydrolase activity	0.032	INM1
YJL198W	PHO90			KRE6
YKL092C	BUD2			SCW11
YLR032W	RAD5			RAD5
YNL168C	FMP41			
YOL092W				
YOR108W	LEU9			
YOR275C	RIM20			
YPR159W	KRE6			
YHR046C				

Table S4: Yeast strains used in this study

strain name	purpose	source
W303 [gar-]		Rothstein
W303 [GAR+]		this study
W303 Δ pma1 pPMA1	genomic copy of pma1 replaced with KanMX, covered by plasmid pPMA1 ura+	this study
W303 Δ rgt2	[GAR+] propagation studies	this study
W303 Δ snf3	[GAR+] propagation studies	this study
W303 Δ yck1	[GAR+] propagation studies	this study
W303 Δ yck2	[GAR+] propagation studies	this study
W303 Δ std1	[GAR+] propagation studies	this study
W303 Δ nth1	[GAR+] propagation studies	this study
W303 Δ rgt1	[GAR+] propagation studies	this study
W303 Δ hxt3	[GAR+] propagation studies	this study
W303 Δ sur4	Pma1 oligomerization studies	this study
W303 Δ lst1	Pma1 oligomerization studies	this study
W303 Δ lcb3	Pma1 oligomerization studies	this study
W303 Δ lcb4	Pma1 oligomerization studies	this study
W303 Δ dpl1	Pma1 oligomerization studies	this study
W303 Δ atg19	Pma1 oligomerization studies	this study
W303 Δ erg5	Pma1 oligomerization studies	this study
W303 GAL- Δ 40N	[GAR+] propagation studies	(Liu and Chang 2006)
W303 GAL- Δ 40N Δ std1	[GAR+] propagation studies	this study
S288c HXT3-GFP	monitoring Hxt3 protein levels in [gar-] and [GAR+]	(Huh et al. 2003)
S288c/W303 HXT3-GFP Δ pma1 pPMA1	monitoring Hxt3 protein levels in [gar-] and [GAR+]	this study

Table S5: Plasmids used in this study

plasmid name	backbone	contains
pPMA1 ura+	pRS316	-1700 to +2950 PMA1
pPMA1 trp+	pRS314	-1700 to +2950 PMA1
pPMA1 S. bay.	pRS314	5' UTR of <i>S. cerevisiae</i> PMA1 (to -1700) fused to <i>S. bayanus</i> PMA1 ORF
pPMA1 S. par.	pRS314	5' UTR of <i>S. cerevisiae</i> PMA1 (to -1700) fused to <i>S. paradoxus</i> PMA1 ORF
pPMA1 S899A	pRS314	pPMA1 mutated at S899
pPMA1 S899D	pRS314	pPMA1 mutated at S899
pPMA1 S911A	pRS314	pPMA1 mutated at S911
pPMA1 S911D	pRS314	pPMA1 mutated at S911
pPMA1 T912A	pRS314	pPMA1 mutated at T912
pPMA1 T912D	pRS314	pPMA1 mutated at T912
pPMA1 911A912A	pRS314	pPMA1 mutated at S911 and T912
pPMA1 911D912D	pRS314	pPMA1 mutated at S911 and T912
pRGT2	p413GPD	RGT2 ORF under control of a GPD promoter (high expression)
pSNF3	p413GPD	SNF3 ORF under control of a GPD promoter
pYCK1	p413GPD	YCK1 ORF under control of a GPD promoter
pYCK2	p413GPD	YCK2 ORF under control of a GPD promoter
pSTD1	p413GPD	STD1 ORF under control of a GPD promoter
pMTH1	p413GPD	MTH1 ORF under control of a GPD promoter
pRGT1	p413GPD	RGT1 ORF under control of a GPD promoter
pHXT3	p413GPD	HXT3 ORF under control of a GPD promoter
pPMA1-OX	p414GPD	PMA1 ORF under control of a GPD promoter
pPMA1 Δ 40N-OX	p414GPD	PMA1 Δ 40N ORF under control of a GPD promoter
pPMA1 Δ 104N-OX	p414GPD	PMA1 Δ 104N ORF under control of a GPD promoter
pPMA1 Δ 40C-OX	p414GPD	PMA1 Δ 40C ORF under control of a GPD promoter
pPMA1Q23stop	p414GPD	pPMA1-OX with nonsense mutation at Q23
pPMA1E59stop	p414GPD	pPMA1-OX with nonsense mutation at E59

Supplemental References

- Amberg, D.C., Burke, D.J., and Strathern, J.N. 2005. *Methods in Yeast Genetics: a Cold Spring Harbor Laboratory Course Manual*. Cold Spring Harbor Laboratory Pres, Cold Spring Harbr.
- Eisenkolb, M., Zenzmaier, C., Leitner, E., and Schneiter, R. 2002. A Specific Structural Requirement for Ergosterol in Long-chain Fatty Acid Synthesis Mutants Important for Maintaining Raft Domains in Yeast. *Mol Biol Cell* **13**(12): 4414-4428.
- Gaigg, B., Timischl, B., Corbino, L., and Schneiter, R. 2005. Synthesis of sphingolipids with very long chain fatty acids but not ergosterol is required for routing of newly synthesized plasma membrane ATPase to the cell surface of yeast. *J Biol Chem* **280**(23): 22515-22522.
- Görg, A., Weiss, W., and Dunn, M.J. 2004. Current two-dimensional electrophoresis technology for proteomics. *Proteomics* **4**(12): 3665-3685.
- Huh, W.-K., Falvo, J.V., Gerke, L.C., Carroll, A.S., Howson, R.W., Weissman, J.S., and O'Shea, E.K. 2003. Global analysis of protein localization in budding yeast. *Nature* **425**(6959): 686-691.
- Liu, Y. and Chang, A. 2006. Quality control of a mutant plasma membrane ATPase: ubiquitylation prevents cell-surface stability. *Journal of cell science* **119**(Pt 2): 360-369.
- Roberg, K.J., Crotwell, M., Espenshade, P., Gimeno, R., and Kaiser, C.A. 1999. LST1 is a SEC24 homologue used for selective export of the plasma membrane ATPase from the endoplasmic reticulum. *The Journal of cell biology* **145**(4): 659-672.
- Schmidt, M.C., McCartney, R.R., Zhang, X., Tillman, T.S., Solimeo, H., Wolf, S., Almonte, C., and Watkins, S.C. 1999. Std1 and Mth1 Proteins Interact with the Glucose Sensors To Control Glucose-Regulated Gene Expression in *Saccharomyces cerevisiae*. *Mol Cell Biol* **19**(7): 4561-4571.

Supplemental Figure Legends

Figure S01: Spontaneous glucosamine-resistant colonies

Exponential phase yeast grown in YPD (2% glucose) were plate to 2% glucose (left) or 2% glycerol + 0.05% glucosamine (GGM; right). Spontaneous glucosamine-resistant colonies are visible on the GGM plate. These are restreaked then used in [*GAR*⁺] studies.

Figure S02: “Strong” and “weak” [*GAR*⁺] strains

a) Spot tests of “strong” and “weak” [*GAR*⁺] strains demonstrate that the different strains result in different colonies sizes on GGM. All plates were incubated at 30°C for the same amount of time. b) “Weak” [*GAR*⁺] diploids result in predominantly “strong” [*GAR*⁺] spores following meiosis (top). A “weak” diploid occasionally gives rise to a four “weak” spores following meiosis (bottom). All spot tests are incubated at 30°C for the same amount of time.

Figure S03: Hsp70-dependent curing of [*GAR*⁺] is reversible

a) The crosses involved in a [*GAR*⁺] propagation assay are shown. Cells carrying [*GAR*⁺] were mated to [*gar*⁻] cells carrying a mutation of interest (“Δ”), here Δ*ssa1*Δ*ssa2*. Diploids were selected for glucosamine-resistance, then sporulated. These spores (“haploids”) were then crossed to wild-type [*gar*⁻] cells and we then selected for the resultant diploids (“diploids”). Both haploids and diploids were tested for glucosamine resistance; if diploids were sensitive to glucosamine, then the [*GAR*⁺] heritable element

cannot be propagated through the mutant of interest and [*GAR*⁺] is therefore “cured” to [*gar*⁻]. b) [*GAR*⁺] frequency within a population of wild-type [*gar*⁻] cells or cells “cured” of [*GAR*⁺] by deletion of *ssa1* and *ssa2*, then crossed to [*gar*⁻]. The final cross to [*gar*⁻] demonstrates whether [*GAR*⁺] can propagate through Δ *ssa1* Δ *ssa2* mutants, as outlined in part a. [*GAR*⁺] frequency is measured in the cells that result from this cross. Because [*GAR*⁺] appears spontaneously at the same frequency as wild-type, Δ *ssa1* Δ *ssa2* mutants reversibly cure [*GAR*⁺]. Also, this demonstrates that [*GAR*⁺] is not “cryptic” in Δ *ssa1* Δ *ssa2* mutants, otherwise all cells would be [*GAR*⁺] and the measured frequency approaching 1.0.

Figure S04: Transcriptional profiling of [*gar*⁻] and [*GAR*⁺] cells

A significance analysis of microarrays (SAM) plot of Affymetrix microarrays comparing [*gar*⁻] and [*GAR*⁺] cells grown in glucose. The X-axis represents the expected difference for each gene between [*gar*⁻] and [*GAR*⁺] and the Y-axis the observed difference. 1000 permutations were run. A single point (green) in the bottom left corner represents the only transcript that exhibits a significant change in abundance: *YDR345C* (*HXT3*).

Figure S05: Knockout mutants of Rgt2/Snf3 pathway members propagate [*GAR*⁺]

[*gar*⁻] strains in which various members of the Rgt2/Snf3 pathway were knocked out were crossed to [*GAR*⁺] cells, then sporulated and dissected. These spores (“1N”) were tested for glucosamine resistance and then crossed to [*gar*⁻] haploids to determine whether [*GAR*⁺] can be propagated through these mutants (“2N”) (see figure S03 for

outline of crosses). $\Delta rgt1$ 1N cells are not glucosamine-resistant but 2N cells are, demonstrating that $[GAR^+]$ is cryptic in $\Delta rgt1$ haploid cells. However, $RGT1$ is not the causal agent of $[GAR^+]$ because $[GAR^+]$ can be propagated from $\Delta rgt1$ to wild-type cells.

Figure S06: Induction of $[GAR^+]$ by $STD1$ and $DOG2$

$STD1$ and $DOG2$ were identified from a screen for genes that induce conversion to $[GAR^+]$ from $[gar^-]$ following transient overexpression. The original screen was performed using a library of plasmids under control of the $GAL1$ promoter. Genes identified during the first round of screen were retested under control of a GPD promoter. $STD1$ and $DOG2$ were identified by this method. $DOG2$ overexpression induces $[GAR^+]$ conversion at a rate 10-fold higher than vector and $STD1$ induces $[GAR^+]$ conversion at a rate over 1000 fold higher than vector. Error bars represent the standard deviation, $n = 6$.

Figure S07: Immunoprecipitation of Std1-6HA from $[gar^-]$ and $[GAR^+]$ cells

Immunoprecipitation of Std1-6HA from $\Delta std1$, $[gar^-]$, and $[GAR^+]$ strains. The total protein lysate is shown on the left and the immunoprecipitation samples on the right. One band (arrow) was found in the immunoprecipitation of Std1-6HA from $[GAR^+]$ but not $[gar^-]$ or $\Delta std1$ samples. This was analyzed by mass spectrometry and found to be Pma1. Coverage was $>20\%$ of the 918 amino acid protein.

Figure S08: Pma1 from $[GAR^+]$ is more sensitive to trypsin than $[gar^-]$ Pma1

Trypsin digestion of Pma1 (left) or Sec61 (right) from $[gar^-]$ (top) or $[GAR^+]$ (middle). A total of six blots were averaged (bottom) and the amount of uncut Pma1 or Sec61 measured and graphed relative to $t = 0$. The graph depicts the mean ($n = 6$) of

($t=n$)/($t=0$) and p-value was calculated using a paired Wilcoxon test. White bars represent [*gar*⁻] protein samples and black bars represent [*GAR*⁺] protein samples. A red asterisks marks statistically significant points ($p = 0.03$).

Figure S09: Δ *sur4* and Δ *lst1* alter Pma1 oligomers but still propagate the [*GAR*⁺] element

a) Native gel blotted for Pma1 from knockout mutants of genes previously shown to affect (Δ *sur4*, Δ *lst1*) (Roberg et al. 1999; Eisenkolb et al. 2002) or not affect (Δ *lcb3*, Δ *lcb4*, Δ *dpl1*) (Gaigg et al. 2005) attributes of wild-type Pma1 (left). SDS gels of total, supernatant (sup.), digitonin soluble (det. sol.), and digitonin insoluble (insol.) fractions were probed with α Pma1 antibody following blotting (right). The “total” blot was also stained with Ponceau Red to confirm equal amounts of starting material (bottom right). b) [*gar*⁻] strains in which either *lst1* (top) or *sur4* (bottom) were knocked out were crossed to [*GAR*⁺] cells, then sporulated and dissected. These spores were tested for glucosamine resistance. All spores grown on glycerol-glucosamine plates, demonstrating that Δ *lst1* and Δ *sur4* can hold [*GAR*⁺]. Δ *sur4* was also identified in our deletion library screen for mutants that exhibit a low frequency of [*GAR*⁺] appearance.

Figure S10: *PMAl* nonsense mutations do not induce [*GAR*⁺]

The *PMAl* ORF containing nonsense mutations at Q23 or E59 was transiently overexpressed. This did not induce [*GAR*⁺] relative to vector, demonstrating that the increase in [*GAR*⁺] due to *PMAl* overexpression (figure 4a) is specific to the Pma1 protein.

Figure S11: PMA1 Δ 40N propagates [GAR⁺]

Top: tetrad spores from a [GAR⁺] diploid with the genotype *GAL-PMA1 Δ 40N/PMA1*. The *pma1* mutation is marked with His⁺. Wild-type spores grown on glucosamine-containing medium but *pma1* mutants cannot grow on any medium lacking galactose, so grown on glycerol-glucosamine cannot be measured. Bottom: spores from top crossed to a [*gar*⁻] strain containing a wild-type *PMA1* allele. *PMA1 Δ 40N* spores grow on glycerol-glucosamine medium and therefore can propagate [GAR⁺] to wild-type [*gar*⁻] yeast.

Figure S12: Pma1 and Std1 do not change localization between [*gar*⁻] and [GAR⁺] cells

a) Detection of Pma1-GFP in [*gar*⁻] and [GAR⁺] cells. Pma1-GFP is found at the plasma membrane and in the vacuole in both [*gar*⁻] and [GAR⁺] cells. These data are supported by the Native gel fractions, which do not show any difference in Pma1 or Std1 between supernatant, soluble, and insoluble fractions (figure 3a). b) Detection of Std1-6HA by indirect immunofluorescence. Std1 was too scarce to be detected by fluorescent protein fusions at the chromosomal locus. Std1-6HA is predominantly in the nucleus in both [*gar*⁻] and [GAR⁺] cells, which is consistent with previous reports (Schmidt et al. 1999).

Figure S13: Pma1 and Std1 do not form SDS-resistant species in [*gar*⁻] or [GAR⁺] cells

a) SDS-treated protein samples from [*psi*⁻] and [*PSI*⁺] (left) and [*gar*⁻] and [GAR⁺] (right) were run on Blue Native gels. Samples were incubated 10min in 4% SDS at 37°C

before running, transferred by standard Western techniques, then probed with α Sup35 (left) or α Pma1 antibodies. Sup35 shows protein in the well in $[PSI^+]$ but not in $[psi^-]$, indicated a difference in SDS-solubility. This is expected because Sup35 forms amyloid in $[PSI^+]$. Pma1, however, does not show any difference in SDS-solubility between $[gar^-]$ and $[GAR^+]$, indicating that Pma1 does not enter into an amyloid state. b) Samples run on SDS gels and blotted for the protein of interest (top) or stained with Ponceau as a loading control (bottom). $[gar^-]$ and $[GAR^+]$ samples were probed with α Pma1 (far left) or α HA (second left; to detect Std1-6HA). There were no differences in mobility in Pma1 or Std1 between $[gar^-]$ and $[GAR^+]$ samples following incubation in 4% SDS for 10min at 37°C. When $[psi^-]$ and $[PSI^+]$ protein samples were treated this way, however, (far right: 37°C for 10min), Sup35 protein from $[PSI^+]$ runs higher than that from $[psi^-]$ and does not resolve well. When protein samples are boiled, however (second right), Sup35 shows no difference in mobility between $[psi^-]$ and $[PSI^+]$. Sup35 therefore behaves like an amyloid in $[PSI^+]$ whereas neither Pma1 nor Std1 exhibit the SDS resistance characteristic of amyloids in $[gar^-]$ or $[GAR^+]$.

Figure S14: $[PSI^+]$, $[URE3]$, and $[RNQ^+]$ do not alter $[GAR^+]$ frequencies

We measured $[GAR^+]$ frequencies in a number of strain backgrounds carrying different states of the PSI, RNQ, and URE3 prions. $[GAR^+]$ frequency varied more with strain background than with prion state of the strain. In the case of the *PSI* prion, strains carrying $[PSI^+]$ sometimes showed a lower $[GAR^+]$ frequency (BY) and sometimes a higher one (W303 and 74D). However, the variation in $[GAR^+]$ frequency in these strains is two fold or less.

Figure S15: 2D gel analysis of [*gar*⁻] and [*GAR*⁺] protein samples does not reveal any proteins that change solubility

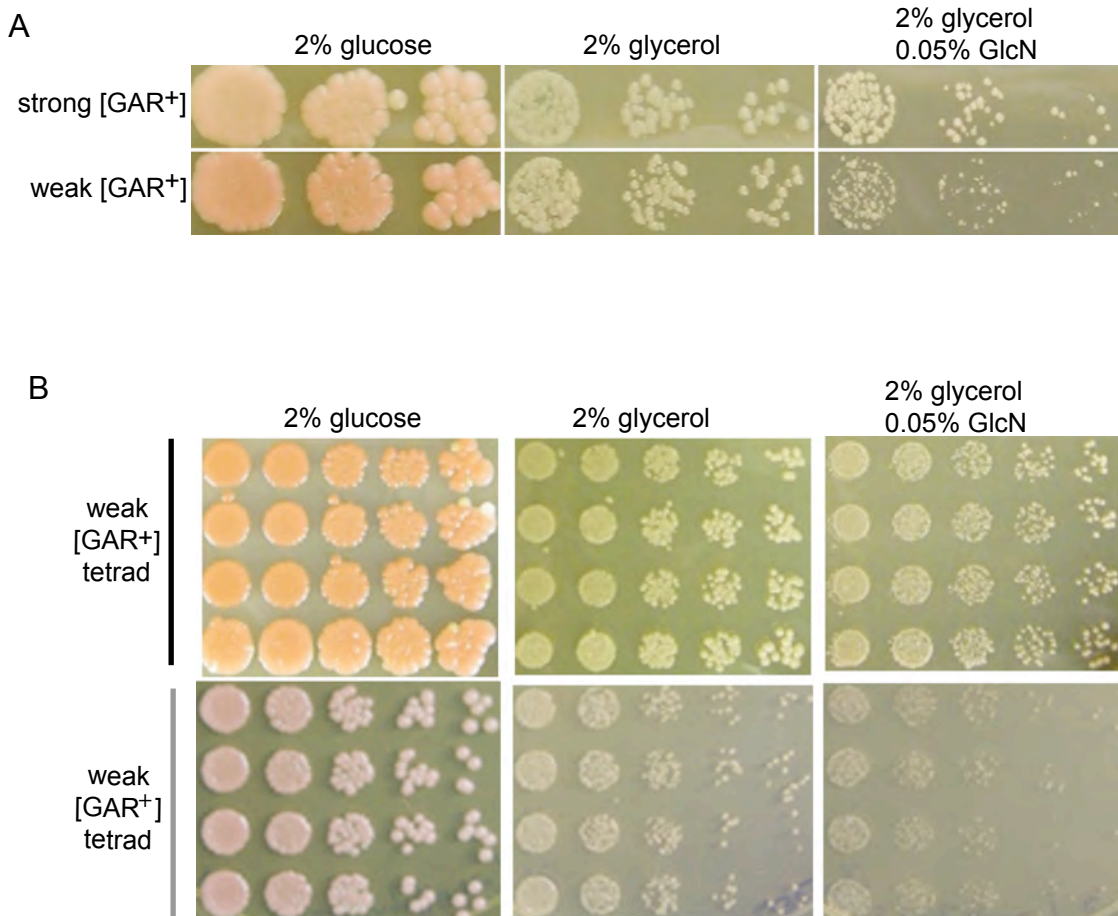
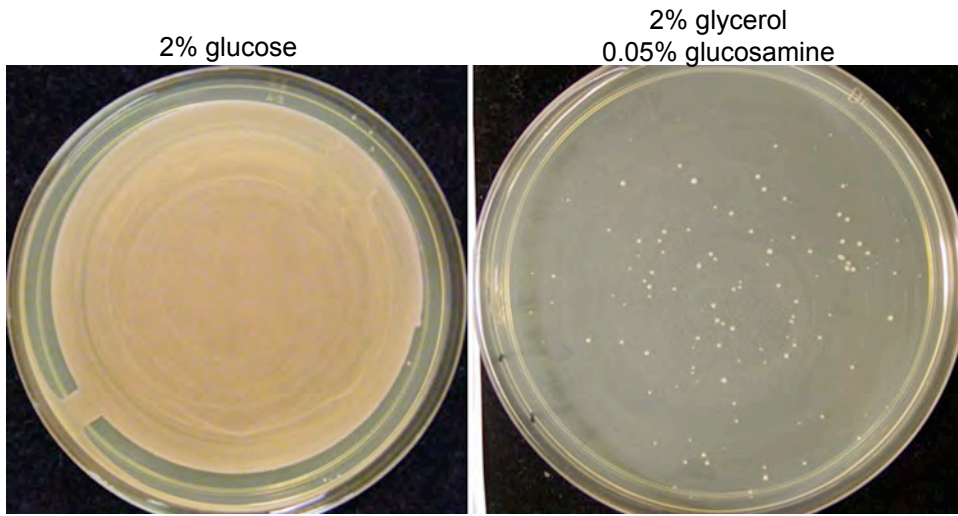
[*gar*⁻] (top) and [*GAR*⁺] (bottom) protein samples were separated into soluble (supernatant; left) and insoluble (pellet; right) fractions, then analyzed by 2D gel electrophoresis. No difference in localization of any protein spot was detected.

Figure S16: Pma1 alignment

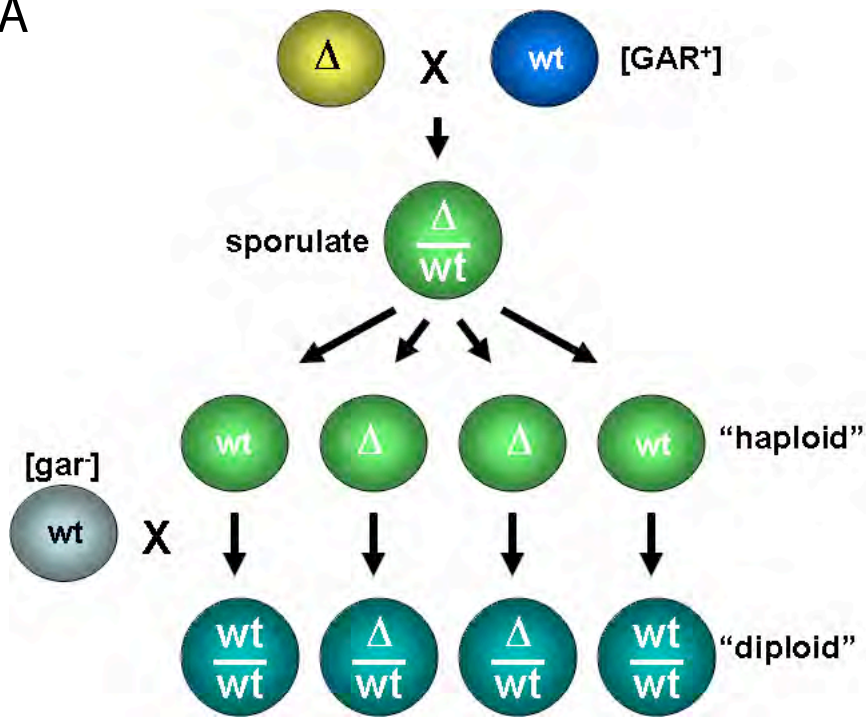
Alignment of Pma1 from *S. cerevisiae*, *S. paradoxus*, and *S. bayanus*. Identical amino acids are marked in blue and different amino acids in red. Red asterisks mark the location of varying amino acids. Red dots mark gaps.

Figure S17: Std1 alignment

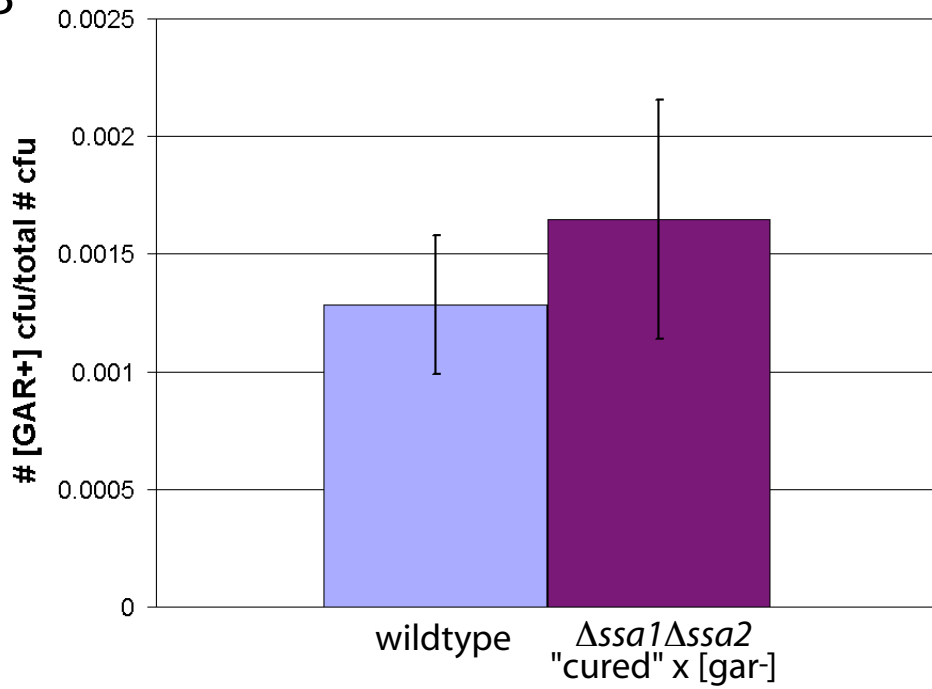
Alignment of Std1 from *S. cerevisiae*, *S. paradoxus*, and *S. bayanus*. Identical amino acids are marked in blue and different amino acids in red. Red asterisks mark the location of varying amino acids. Red dots mark gaps. Note that the N-terminus of *S. paradoxus* Std1 is missing.

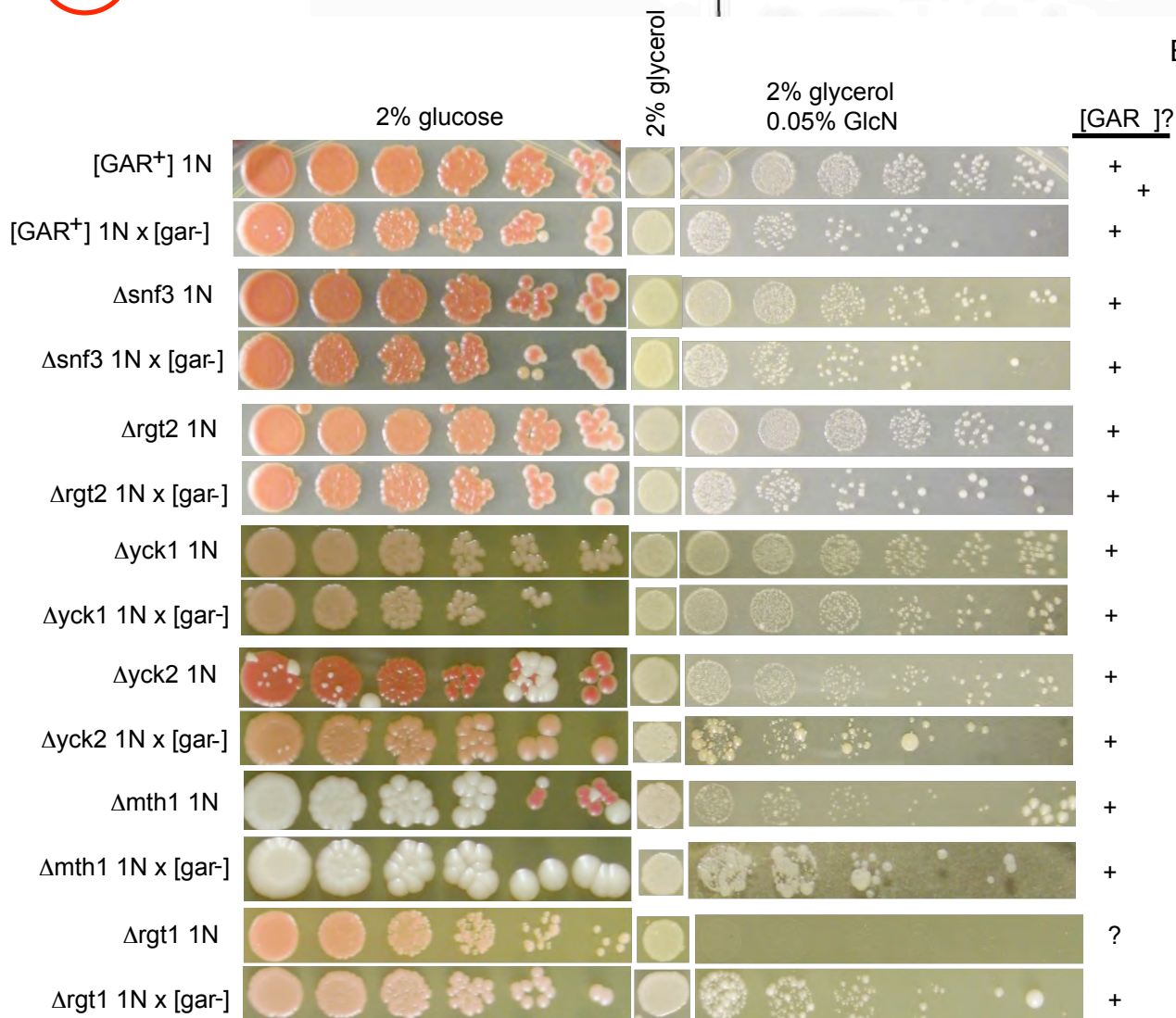
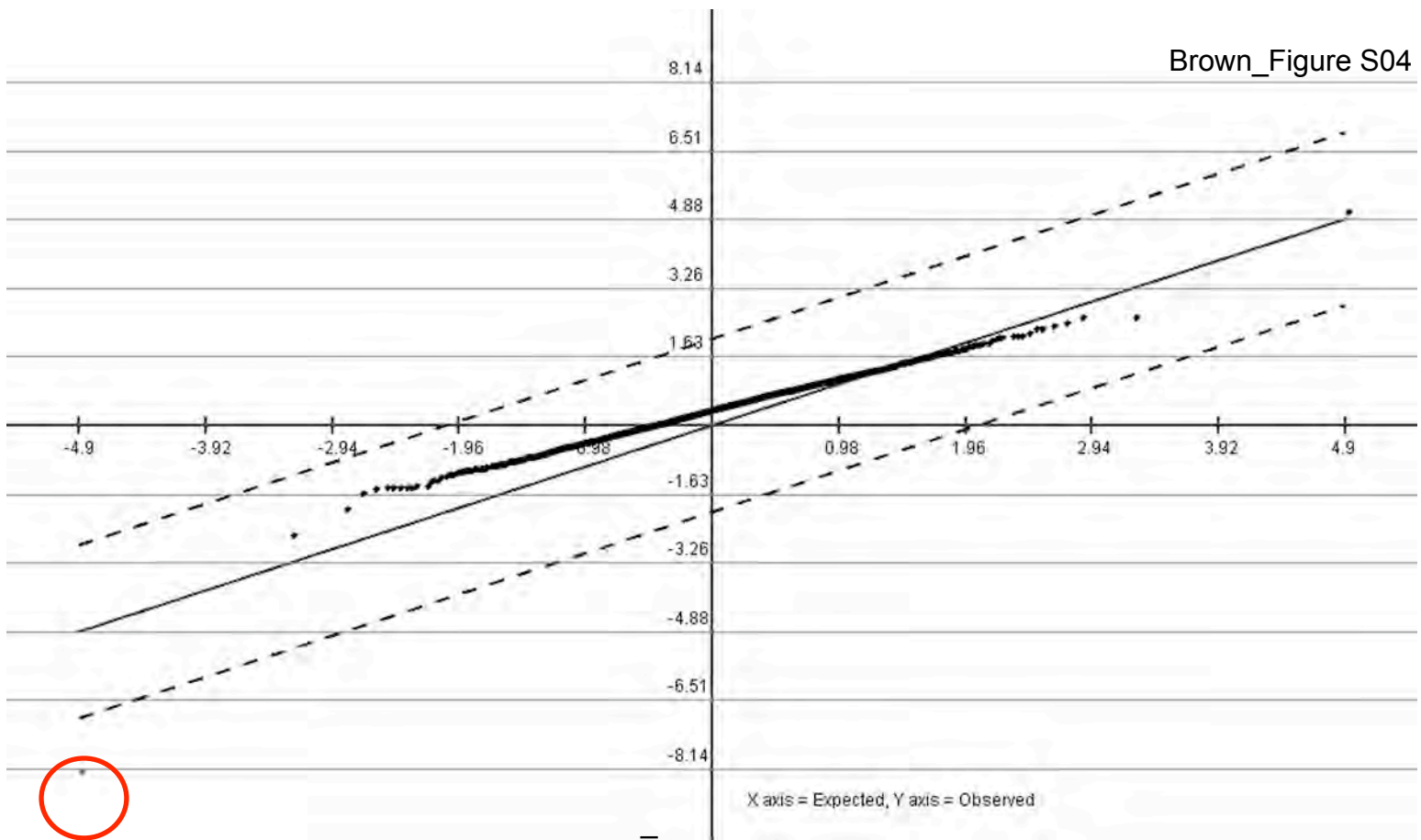


A

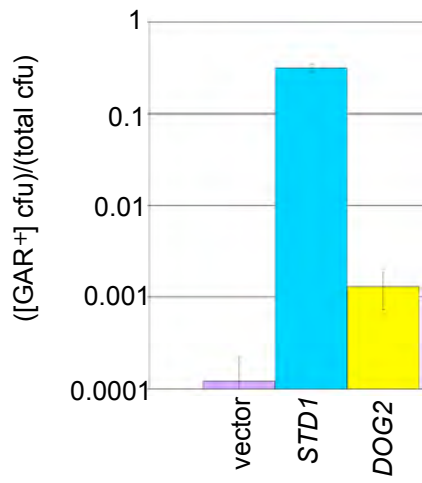


B

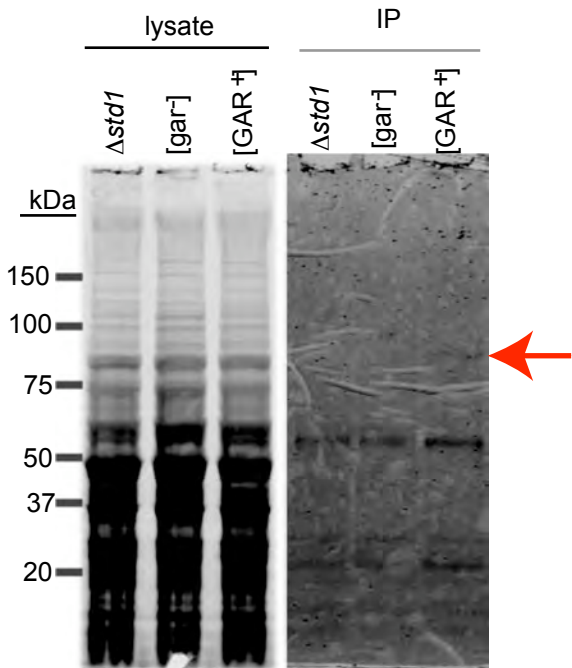


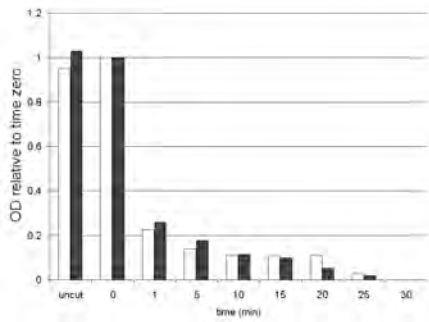
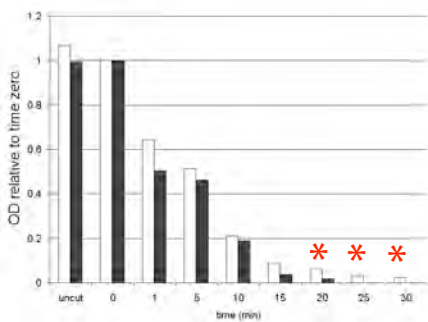
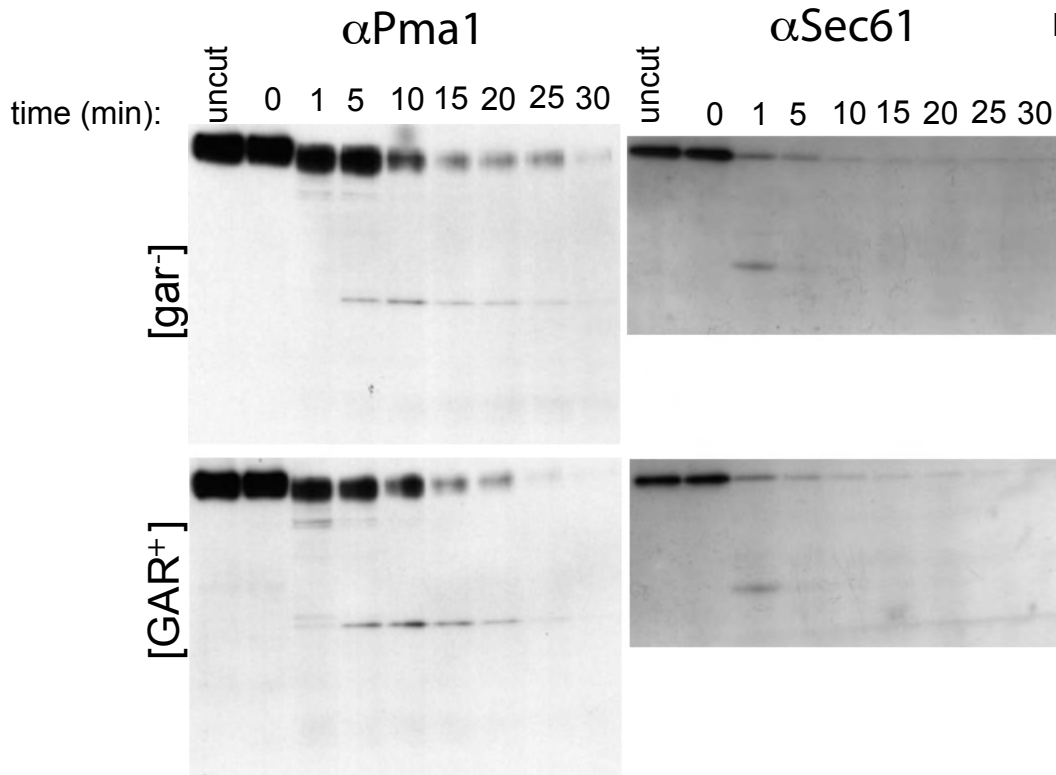


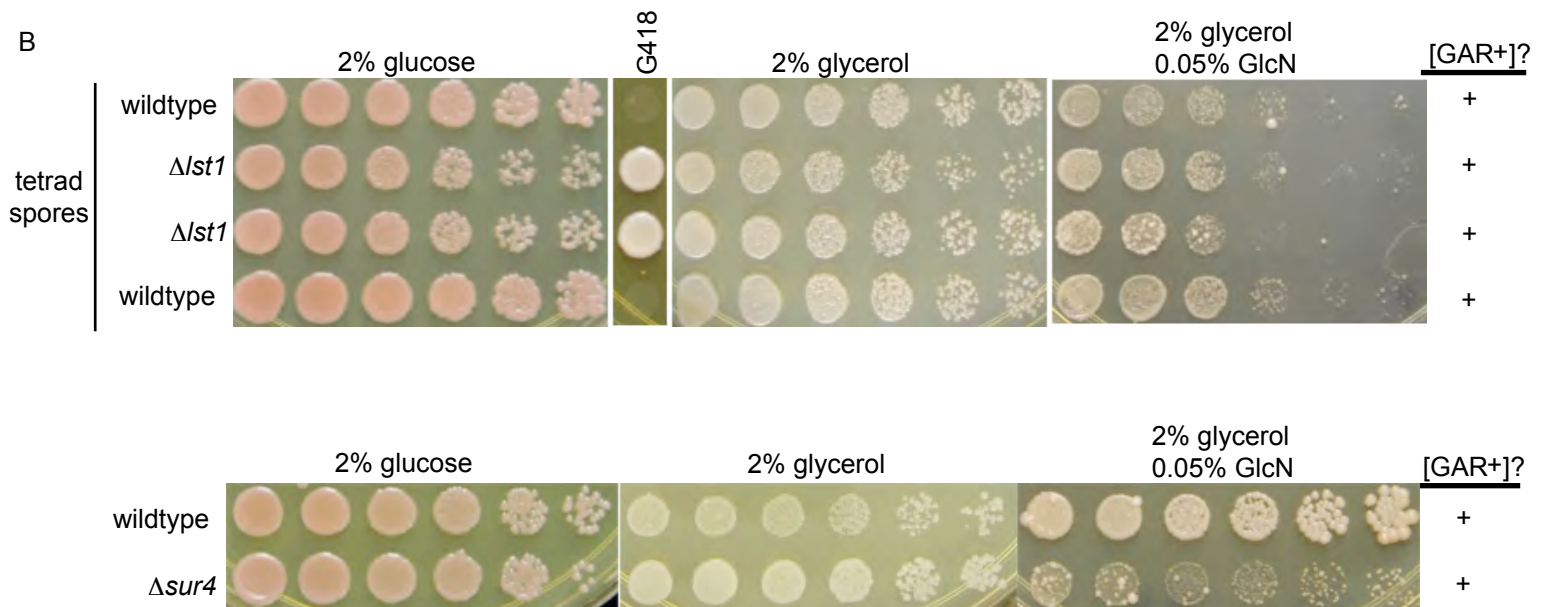
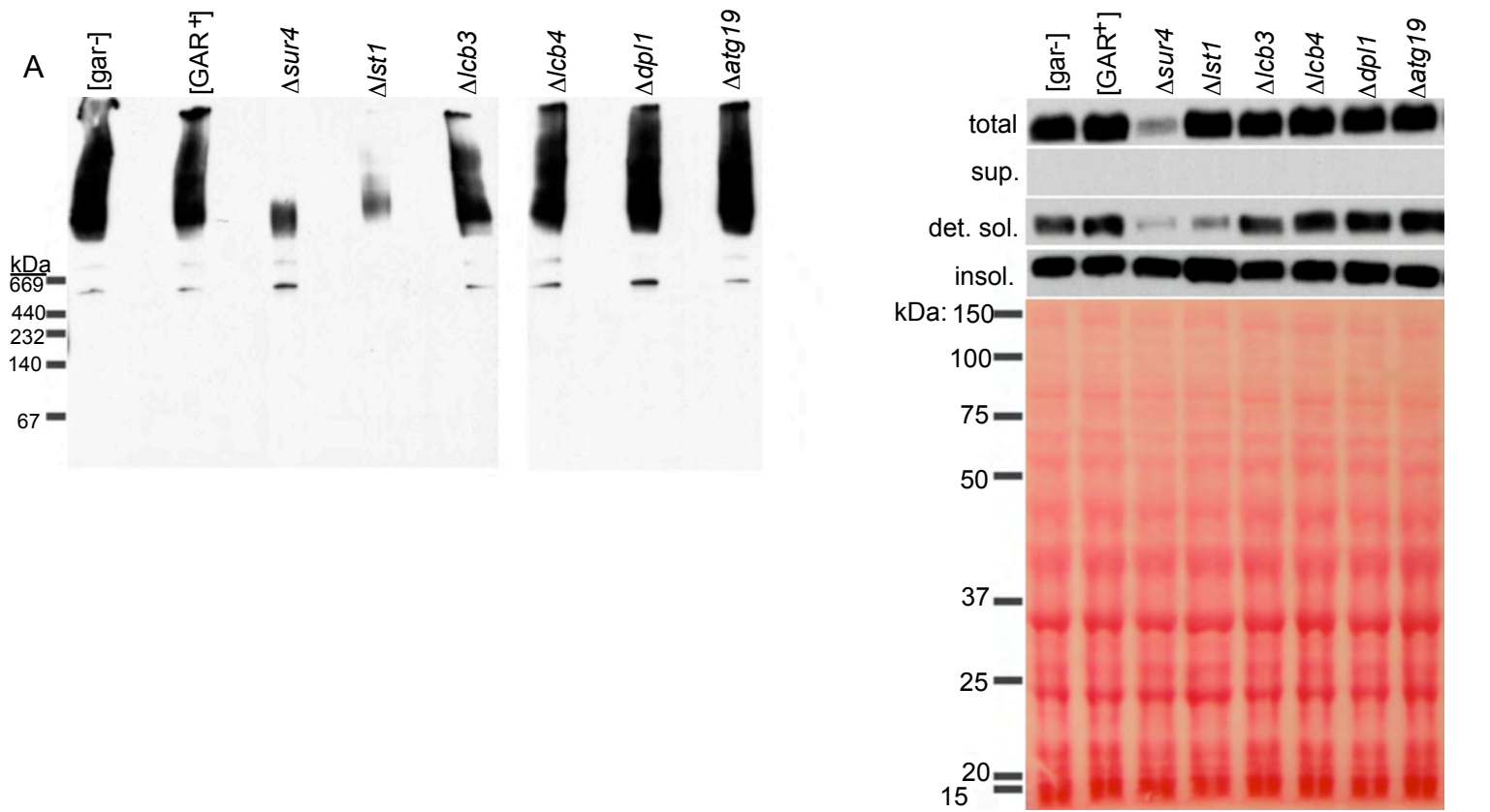
Brown_Figure S06



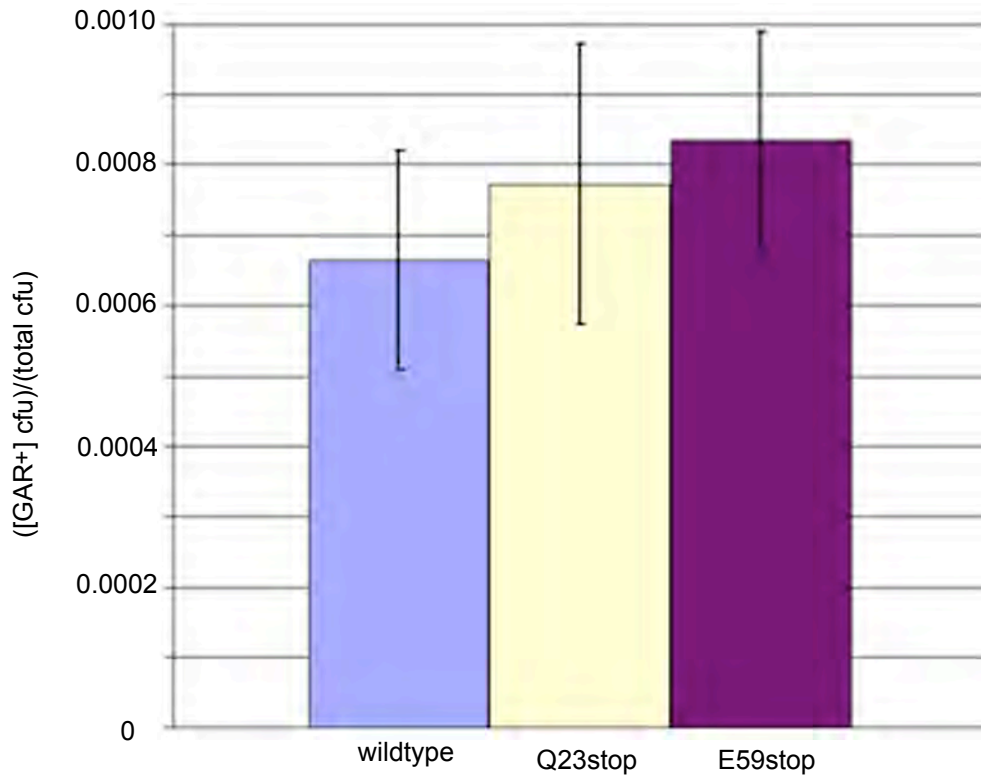
Brown_Figure S07



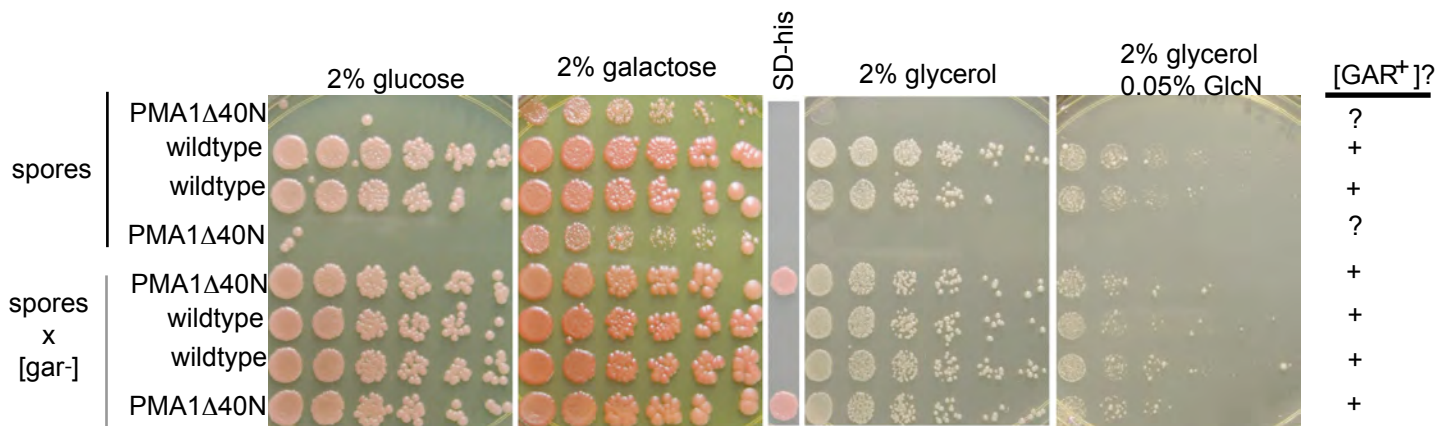


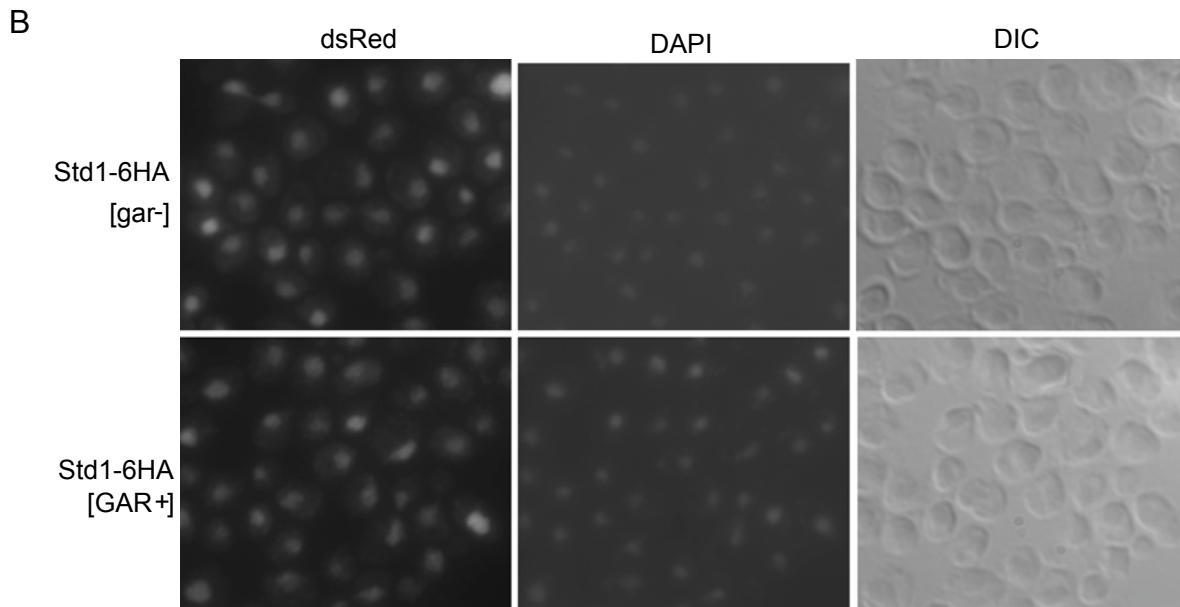
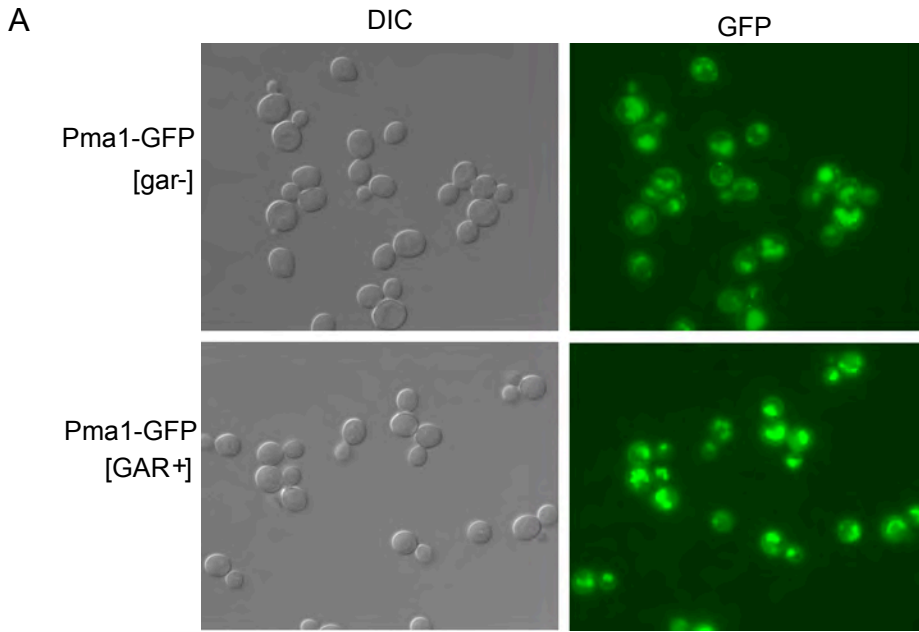


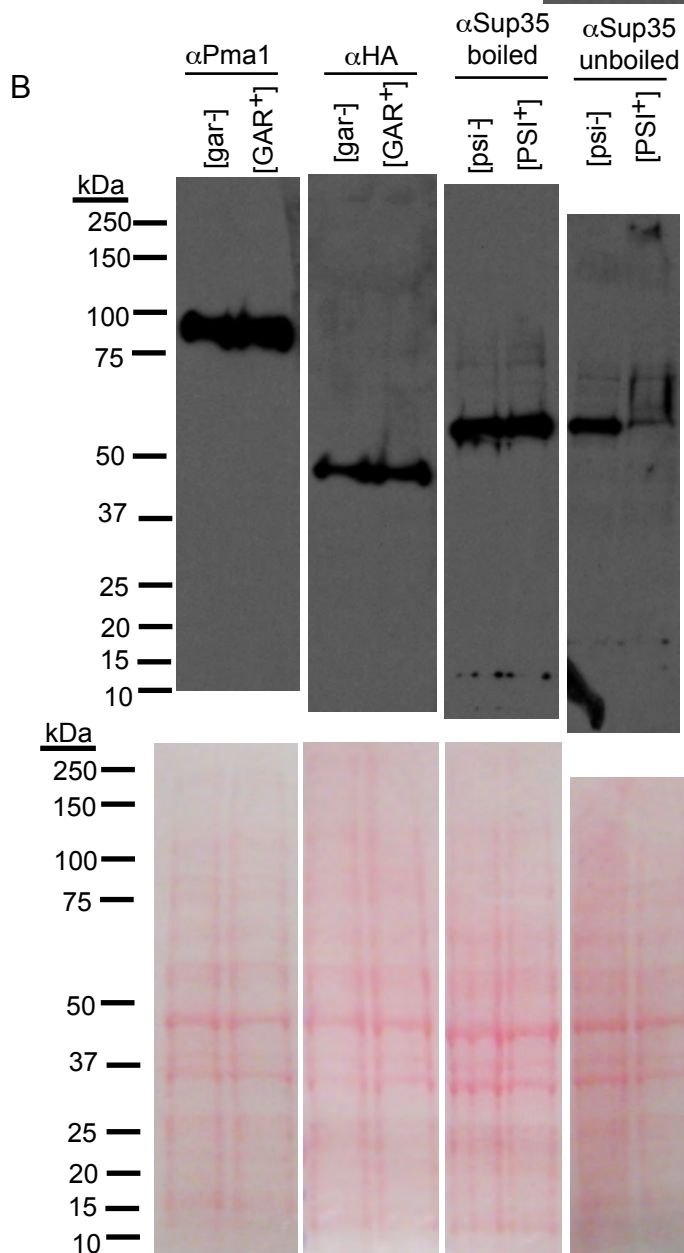
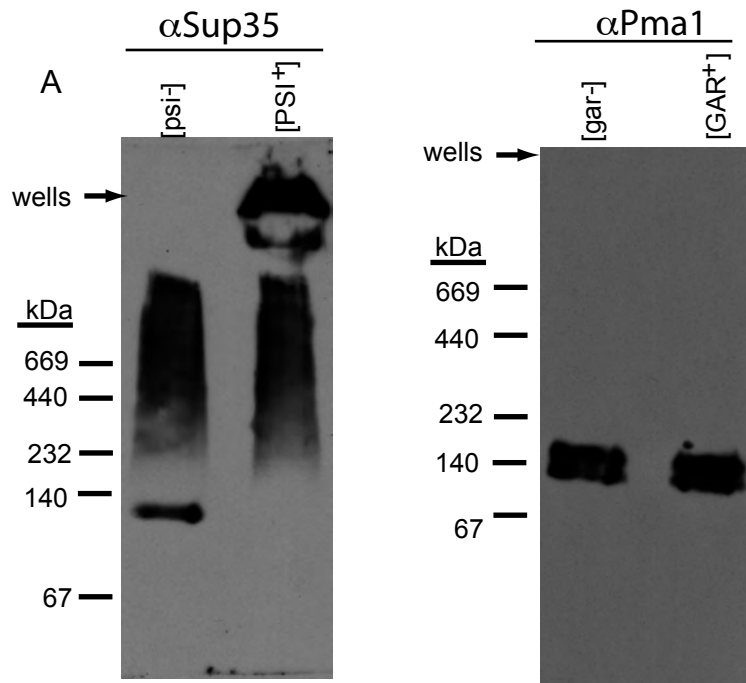
Brown_Figure S10



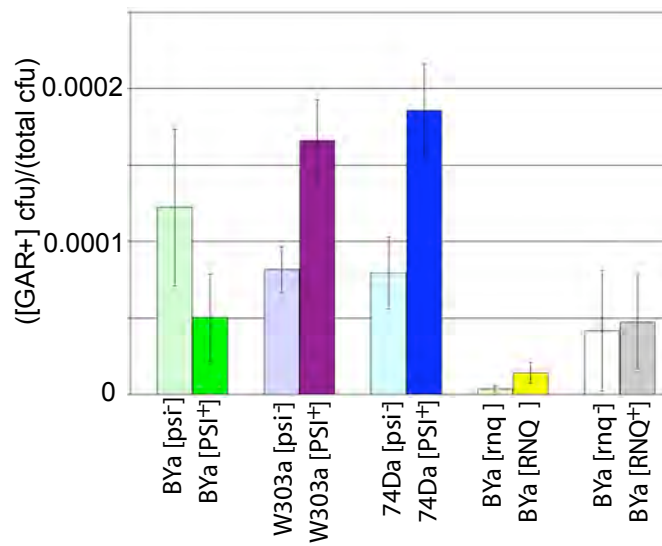
Brown_Figure S11



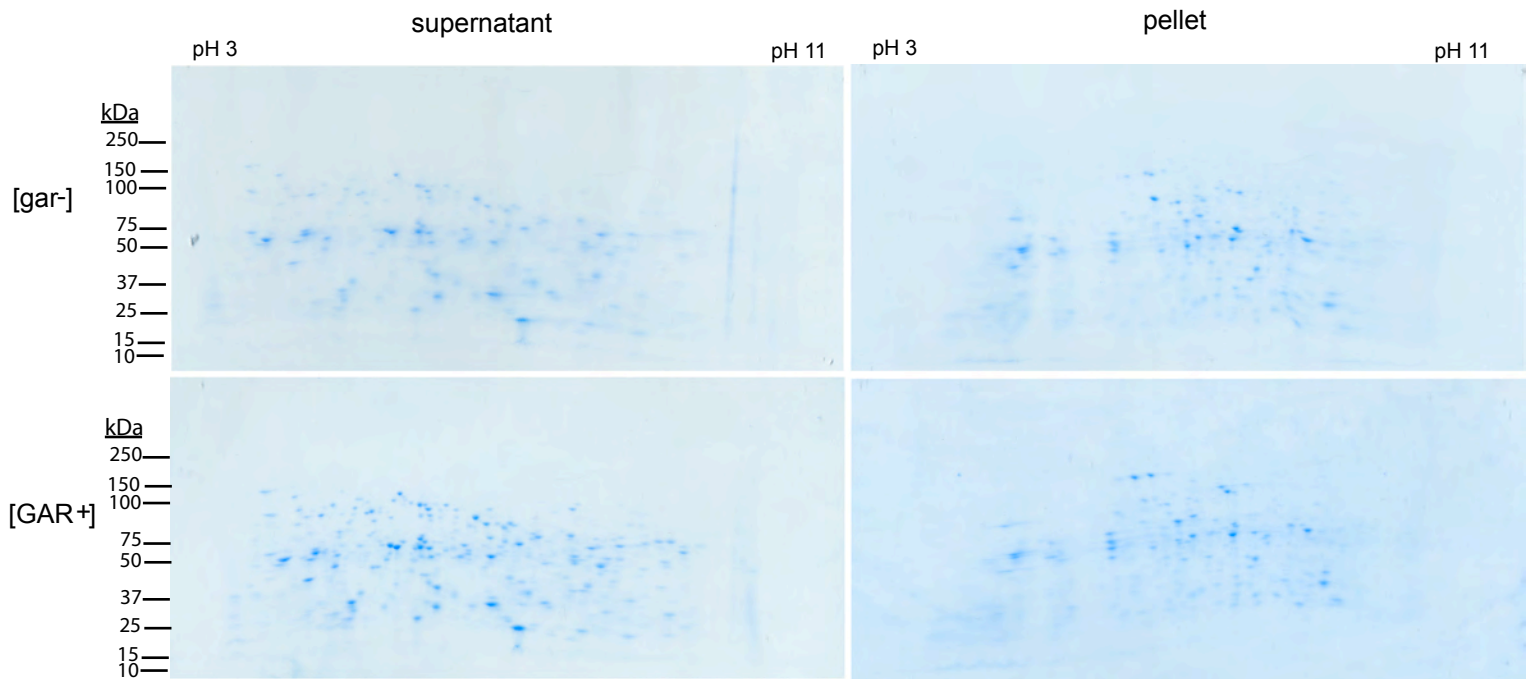




Brown_Figure S14



Brown_Figure S15



Brown_Figure S16

	1	* * * * *	* *		*		50
Scer	MTDTSSSSSS	SS	.ASSVSAH	QPTQEKPAKT	YDDAAESSD	DDDIDALIEE	
Spar	MADTSSSSSS	SSS	ASSVSAH	QPTQEKPAKT	YDDAAESSD	DDDIDALIEE	
Sbay	...MTDNTSS	SSS	ASSASA	QPTQEKPAKT	FDDAAESSD	DDDIDALIDE	
	51	* ** * **		* *			100
Scer	LQSNHGVDDE	DSD	NDGPVAA	GEARVPPEEY	LQTDPSYGLT	SDEVLKRRKK	
Spar	LQSNHGVDDE	GSD	DDGPVAA	GEARVPPEEY	LQTDPSYGLT	SDEVLKRRKK	
Sbay	LQSNPGVDGS	ESE	DDGPVAA	GEARLVPEEL	LQTDPSYGLT	SDEVLKRRKK	
	101	*** ** *					150
Scer	YGLNQMADEK	ESL	VVKFVMF	FVGPIQFVME	AAAILAAGLS	DWVDFGVICG	
Spar	YGLNQMADEK	ESL	VVKFVMF	FVGPIQFVME	AAAILAAGLS	DWVDFGVICG	
Sbay	YGLNQMAENN	ESL	IKFIMF	FVGPIQFVME	AAAILAAGLS	DWVDFGVICG	
	151		*		*		200
Scer	LLMLNAGVGF	VQE	FQAGSIV	DELKKTANT	AVVIRDGQLV	EIPANEVVPG	
Spar	LLMLNAGVGF	VQE	FQAGSIV	DELKKTANT	AVVIRDGQLV	EIPANEVVPG	
Sbay	LLMLNAGVGF	IQE	FQAGSIV	EELKKTANT	AVVIRDGQLV	EIPANEVVPG	
	201						* 250
Scer	DILQLEDGTV	IPT	DGRIVTE	DCFLQIDQSA	ITGESLAVDK	HYGDQTFSSS	
Spar	DILQLEDGTI	IPT	DGRIVTE	DCFLQIDQSA	ITGESLAVDK	HYGDQTFSSS	
Sbay	DILQLEDGTI	IPT	DGRIVTE	ECFLQIDQSA	ITGESLAVDK	HYGDQAFSSS	
	251				*		300
Scer	TVKRGEFVMV	VTAT	GDNTFV	GRAAALVNKA	AGGQGHFTEV	LNGIGIILLV	
Spar	TVKRGEFVMV	VTAT	GDNTFV	GRAAALVNKA	AGGQGHFTEV	LNGIGIILLV	
Sbay	TVKRGEFVMV	VTAT	GDNTFV	GRAAALVNKA	SGGQGHFTEV	LNGIGIILLV	
	301	* *					350
Scer	LVIATLLLVW	TAC	FYRTNGI	VRILRYTLGI	TIIGVPVGLP	AVVTTTMAVG	
Spar	LVVATLLLVW	TAC	FYRTNGI	VRILRYTLGI	TIIGVPVGLP	AVVTTTMAVG	
Sbay	LVIITLLVW	TAC	FYRTNGI	VRILRYTLGI	TIIGVPVGLP	AVVTTTMAVG	
	351						400
Scer	AAYLAKKQAI	VQK	LSAIESL	AGVEILCSDK	TGTLTKNKLS	LHEPYTVEGV	
Spar	AAYLAKKQAI	VQK	LSAIESL	AGVEILCSDK	TGTLTKNKLS	LHEPYTVEGV	
Sbay	AAYLAKKQAI	VQK	LSAIESL	AGVEILCSDK	TGTLTKNKLS	LHEPYTVEGV	
	401				*		450
Scer	SPDDLMLTAC	LAAS	RKKKGL	DAIDKAFLKS	LKQYPAKDA	LTKYKVLEFH	
Spar	SPDDLMLTAC	LAAS	RKKKGL	DAIDKAFLKS	LKQYPAKDA	LTKYKVLEFH	
Sbay	SADDLMLTAC	LAAS	RKKKGL	DAIDKAFLKS	LIQYPAKDA	LTKYKVLEFH	
	451						500
Scer	PFDPVSKKVT	AVVE	SPEGER	IVCVKGAPLF	VLKTVEEDHP	IPEDVHENYE	
Spar	PFDPVSKKVT	AVVE	SPEGER	IVCVKGAPLF	VLKTVEEDHP	IPEDVHENYE	
Sbay	PFDPVSKKVT	AVVE	SPEGER	IVCVKGAPLF	VLKTVEEDHP	IPEDVHENYE	

	501					550
Scer	NKVAELASRG	FRALGVARKR	GEGHWEILGV	MPCMDPPRDD	TAQTVSEARH	
Spar	NKVAELASRG	FRALGVARKR	GEGHWEILGV	MPCMDPPRDD	TAQTVSEARH	
Sbay	NKVAELASRG	FRALGVARKR	GEGHWEILGV	MPCMDPPRDD	TAQTVSEARH	
	551					600
Scer	LGLRVKMLTG	DAVGIAKETC	RQLGLGTNIY	NAERLGLGGG	GDMPGSELAD	
Spar	LGLRVKMLTG	DAVGIAKETC	RQLGLGTNIY	NAERLGLGGG	GDMPGSELAD	
Sbay	LGLRVKMLTG	DAVGIAKETC	RQLGLGTNIY	NAERLGLGGG	GDMPGSELAD	
	601					650
Scer	FVENADGFAE	VFPQHKYRVV	EILQNRGYLV	AMTGDGVNDA	PSLKKADTGI	
Spar	FVENADGFAE	VFPQHKYRVV	EILQNRGYLV	AMTGDGVNDA	PSLKKADTGI	
Sbay	FVENADGFAE	VFPQHKYRVV	EILQNRGFLV	AMTGDGVNDA	PSLKKADTGI	
	651					700
Scer	AVEGATDAAR	SAADIVFLAP	GLSAIIDALK	TSRQIFHRMY	SYVVYRIALS	
Spar	AVEGATDAAR	SAADIVFLAP	GLSAIIDALK	TSRQIFHRMY	SYVVYRIALS	
Sbay	AVEGATDAAR	SAADIVFLAP	GLSAIIDALK	TSRQIFHRMY	SYVVYRIALS	
	701		*			750
Scer	LHLEIFLGLW	IAILDNSLDI	DLIVFIAIFA	DVATLAIAYD	NAPYSPKPVK	
Spar	LHLEIFLGLW	IAILDNSLNI	DLIVFIAIFA	DVATLAIAYD	NAPYSPKPVK	
Sbay	LHLEIFLGLW	IAILDNSLDI	DLIVFIAIFA	DVATLAIAYD	NAPYSPKPVK	
	751		* *			800
Scer	WNLPRLWGMS	IILGIVLAIG	SWITLTTMFL	PKGIIQNF	AMNGIMFLQI	
Spar	WNLPRLWGMS	IILGIVLAVG	SWITLTTMFL	PKGIIQNF	ALNGIMFLQI	
Sbay	WNLPRLWGMS	IILGIVLAVG	SWITLTTMFL	PKGIIQNF	AMNGIMFLQI	
	801		*			850
Scer	SLTENWLIFI	TRAAGPFWSS	IPSWQLAGAV	FAVDIIATMF	TLFGWSENW	
Spar	SLTENWLIFI	TRAAGPFWSS	IPSWQLAGAV	FAVDIIATMF	TLFGWSENW	
Sbay	SLTENWLIFI	TRAAGPFWSS	VPSWQLAGAV	FAVDIIATMF	TLFGWSENW	
	851			*	*	900
Scer	TDIVTVVRVW	IWSIGIFCVL	GGFYEMSTS	EAFDRLMNGK	PMKEKKSTRS	
Spar	TDIVTVVRVW	IWSIGIFCVL	GGFYEMSTS	EAFDRVMNGK	PMKEKKSTRS	
Sbay	TDIVTVVRVW	IWSIGIFCVL	GGFYEMSTS	EAFDRMMNGK	PAKEKKSTRS	
	901		919			
Scer	VEDFMAAMQR	VSTQHEKET				
Spar	VEDFMAAMQR	VSTQHEKET				
Sbay	VEDFLAAMQR	VSTQHEKEA				

Brown_Figure S17

	1	*****	*****	*****	*****	*****	50
Scer		MFVSPPPATA	RNQVLGKRKS	KRHDENPKNV	QPNADTEMTN	SVPSIGFNSN	
Sbay		MFVSPPPATA	RNQVLGKRKS	KRRGSNSKNV	QPISNSPDVD	KSVSFVPNNH	
Spar		
	51	*****	*****	*****	*****	*****	100
Scer		LPHNNQEINT	PNHYNLSSNS	GNVRSNNNFV	TTPPEYADRA	RIEIIKRLLP	
Sbay		PSYSEQEANT	PNHYSLNASP	GNSRSN..FV	STPPEYADRA	RIEIRKRLLP	
Spar		
	101	*****	*****	*****	*****	*****	150
Scer		TAGTKPMEVN	SNTAENANIQ	HINTPDSQSF	VSDHSSSYES	SIFSQPSTAL	
Sbay		TGGNKPISVN	SVFLDNANIH	QVTSPDSQSF	VSDQASSYES	SIFSHPSTVL	
Spar		
	151	*****	*****	*****	*** *		200
Scer		TDITTGSSLI	DKTKPKFVTE	VTLEDALPKT	FYDMYSPEVL	MSDPANILYN	
Sbay		TRVTTDSSLI	DLKTKPKFVTE	ITLEDALPKT	FYDMYTPEVL	MSDPANILYN	
Spar	MYSPEVL	MSDPANILYN	
	201			*	* *		250
Scer		GRPKFTKREL	LDWDLNDIRS	LLIVEQLRPE	WGSQLPTVVT	SGINLPQFRL	
Sbay		GRPKFTKREL	LDWDLNDIRS	LLIVERLRPE	WGSRLPSVIT	SGINLPQFRL	
Spar		GRPKFTKREL	LDWDLNDIRS	LLIVEQLRPE	WGSQLPTVVT	SGINLPQFRL	
	251	*		*			300
Scer		QLLPLSSSDE	FIIATLVNSD	LYIEANLDRN	FKLTSAKYTV	ASARKRHEEM	
Sbay		QLLPLCSSDE	FIIATLVNSD	LYIEANLDRD	FKLTSAKYTV	ASARKRHEEI	
Spar		QLLPLRSSDE	FIIATLVNSD	LYMEANLDRN	FKLTSAKYTV	ASARKRHEEM	
	301	* *				*	350
Scer		TGSKEPIMRL	SKPEWRNIIE	NYLLNVAVEA	QCRYDFKQKR	SEYKRWKLLN	
Sbay		VGYNETIMRL	SKPEWRNIIE	NYLLNVAVEA	QCRYDFKQKR	SEYKKWKQLN	
Spar		TGSNEPIMRL	SKPEWRNIIE	NYLLNVAVEA	QCRYDFKQKR	SEYKRWKLLN	
	351		** **	***	*		*400
Scer		SNLKRPMPP	PSLIPHGFKI	HDCTNSGSLI	KKALMKNLQL	KNYKNDAKTL	
Sbay		SNLKRPMPP	PSLIPPDFHT	HEHISSGSLI	KKALMKNLQL	KNYKNDTKTL	
Spar		SNLKRPMPP	PSLIPHGFLA	HDCANSGSLI	KKALIKNLQL	KNYKNDAKAL	
	401		*	* *		*	444
Scer		GAGTQKNVVN	KVSLTSEERA	AIWFQCQTQV	YQRLGLDWKP	DGMS	
Sbay		GAGTQKNVVN	KVSLTKEERA	GIWLQCQTQV	YQRLGLDWTP	DGMS	
Spar		GAGTQKNVVN	KVSLTSEERA	AIWFQCQTQV	YQRLGLDWKP	DKMS	